Eco-Friendly Intelligent Transportation System Technology for Freight Vehicles

| March 2017 | A Research Report from the National Center for Sustainable Transportation |

David Kari, CE-CERT at UC Riverside

Guoyuan Wu, CE-CERT at UC Riverside

Matthew Barth, CE-CERT at UC Riverside

National Center for Sustainable Transportation

UCR | College of Engineering- Center for Environmental Research & Technology

About the National Center for Sustainable Transportation

The National Center for Sustainable Transportation is a consortium of leading universities committed to advancing an environmentally sustainable transportation system through cutting-edge research, direct policy engagement, and education of our future leaders. Consortium members include: University of California, Davis; University of California, Riverside; University of Southern California; California State University, Long Beach; Georgia Institute of Technology; and University of Vermont. More information can be found at: http://ncst.ucdavis.edu.

U.S. Department of Transportation (USDOT) Disclaimer

The contents of this report reflect the views of the authors, who are responsible for the facts and the accuracy of the information presented herein. This document is disseminated under the sponsorship of the United States Department of Transportation's University Transportation Centers program, in the interest of information exchange. The U.S. Government assumes no liability for the contents or use thereof.

Acknowledgments

Eco-Friendly Intelligent Transportation System Technology for Freight Vehicles

A National Center for Sustainable Transportation Research Report

March 2017

David Kari, Center for Environmental Research and Technology, University of California, Riverside

Guoyuan Wu, Center for Environmental Research and Technology, University of California, Riverside

Matthew Barth, Center for Environmental Research and Technology, University of California, Riverside

[page left intentionally blank]

TABLE OF CONTENTS

Eco-Friendly Intelligent Transportation System Technology for Freight Vehicles

EXECUTIVE SUMMARY

Heavy-duty freight vehicles contribute a disproportionate amount of emissions relative to the national fleet percentage and the relative vehicle miles traveled by heavy-duty freight vehicles. Accordingly, an environmentally-friendly Intelligent Transportation System (ITS) application for improving arterial roadway performance is presented in this report. For arterial roadways, most Active Traffic and Demand Management (ATDM) strategies focus on traffic signal timing optimization at signalized intersections. A critical drawback of conventional traffic signal control strategies is that they rely on measurements from point detection, and estimate traffic states such as queue length based on very limited information. The introduction of Connected Vehicle (CV) technology can potentially address the limitations of point detection via wireless communications to assist signal phase and timing optimization. In this project report, we present an agent-based online adaptive signal control (ASC) strategy based on real-time traffic information available from vehicles equipped with CV technology. We then evaluate the proposed strategy in terms of travel delay and energy consumption, relative to a Highway Capacity Manual (HCM) based method in which hourly traffic demand is assumed to be known accurately *a priori*. This Connected Vehicle Adaptive Signal Control (CV-ASC) strategy has been applied to an isolated traffic intersection as well as to a corridor of traffic intersections. The baseline signalization strategy for the corridor of traffic intersections is coordinated signal control. Study results indicate that for both the isolated intersection and corridor contexts, the proposed strategy outperforms the HCM based method and is very robust to traffic demand variations. The proposed system also provides a framework to flexibly modify signal timing in order to serve evolving localities freight needs.

1. Introduction

In most urban areas, travel demand continues to grow, coupled with limited capacity expansion of existing roadway facilities. As a result, a variety of challenges have emerged, including ever-increasing congestion, along with higher energy consumption and pollutant emissions. Based on the latest Urban Mobility Report (UMR) [1], traffic congestion caused 5.5 billion hours of travel delays and approximately 2.9 billion gallons of unnecessary fuel consumption across 498 urban areas in the United States. In addition, the U.S. Environmental Protection Agency (USEPA) has estimated that the transportation sector contributed about 34.4% of total U.S. carbon dioxide (CO2) emissions and 28.2% of total U.S. greenhouse gas (GHG) emissions in 2012 [2]. Furthermore, heavy-duty freight vehicles contributed 21.9% of transportation sector GHG emissions in 2012 [2], despite accounting for only 9.2% of vehicle miles traveled [3]. Accordingly, one of the goals of Intelligent Transportation System research is to provide eco-friendly solutions for reducing the disproportionate environmental impact of heavy-duty freight vehicles. Strategies may be applied to improve environmental performance in the context of freeways or arterial intersections. This report focuses on improving the environmental performance of vehicles near arterial intersections.

Due to the significant costs of expanding the existing infrastructure, developing Active Traffic and Demand Management (ATDM) strategies, which aim at maximizing the utilization of existing roadway resources, has proven to be an attractive solution to the problems associated with traffic congestion in urban areas. For arterial roadways, most ATDM strategies have focused on signal timing optimization at signalized intersections or along signalized corridors, with the goal of determining the best cycle lengths, green splits, phase sequences, and offsets to favor traffic operation. Although a variety of optimal traffic signal control strategies have been proposed over the decades, most of them are essentially "off-line" or designed for pre-timed signal control without considering transition between pre-set plans [4]. Usually, the existing ATDM strategies assume that the traffic demand on each intersection approach is known and steady during the analysis period (e.g., one hour or morning peak). Thus, the system performance degrades significantly under variations in real-world traffic conditions. As traffic surveillance technologies have advanced, traffic responsive signal control systems have become wide-spread; nevertheless, most of them rely on very limited information, such as passage or presence of a vehicle, available from point detection (e.g., from inductive loop detectors or ILDs) [5], sometimes giving rise to unsatisfactory system performance.

The introduction of wireless communication among vehicles (V2V), as well as between vehicles and infrastructure (V2I/I2V), referred to as Connected Vehicle (CV) technology, provides a well-defined platform for continuously monitoring vehicles' characteristics (e.g., vehicle type) and activities (e.g., location and speed). With comprehensive information on real-time traffic conditions provided by CV technology, many potential problems associated with conventional point detection can be addressed.

In this project report, we focus on improving arterial traffic light signal control as a means of reducing freight vehicle emissions in urban areas. An online adaptive traffic signal control (ATSC) strategy based on CV technology is proposed, which is capable of adjusting traffic light settings, including green splits and phase sequence, in response to the variations in traffic demand and arrival pattern such that the system-wide measures of effectiveness (e.g., travel delay and fuel consumption) can be significantly reduced. The remainder of this report is organized as follows: the next section introduces background information for the development and evaluation of the proposed CV technology based ATSC algorithm. Chapter 3 presents the detailed description of the proposed algorithm applied to an isolated traffic intersection. In chapter 4, the algorithm is extended to operate on a corridor of traffic signals. Case studies and sensitivity analyses are included in chapters 3 and 4, followed by the conclusions in chapter 5 and a discussion of future work.

2. Background

2.1 Connected Vehicles

The term "Connected Vehicles" (CVs) is used in the field of Intelligent Transportation Systems (ITS) to refer to vehicles that are equipped to communicate with and receive information from other vehicles and infrastructure. The "connection" portion of CV consists of the sharing and exchange of information. The communication involving CVs is categorized into several types including vehicle-to-vehicle communication (V2V), vehicle-to-infrastructure communication (V2I), and infrastructure-to-vehicle communication (I2V). Each of the categories is implemented using wireless communication. The two primary technologies most often considered for enabling wireless communication to and from vehicles are Dedicated Short Range Communication for Wireless Access in Vehicular Environments (DSRC/WAVE) radios and cellular communication devices. Referred to as DSRC for short, DSRC operates within a 75 MHz range in the 5.9 GHz band, as set forth by the Federal Communications Commission (FCC) in Report and Order FCC-03-324 [6]. DSRC has the advantage of using standardized message formats, which enhance interoperability. Example message formats include the Basic Safety Message (BSM) (parts I and II), as standardized in the SAE J2735 standard. Additional advantages of DSRC include relatively low latency and high reliability including under adverse weather conditions. One of the drawbacks of DSRC is its communication range, which is typically set to 300 meters, though ranges of up to 1000 meters are possible [7]. In contrast, cellular devices have a greater range, but are less reliable and are not designed specifically for vehicle safety applications. However, cellular devices can be used to augment DSRC with non-critical information such as traffic conditions 10 miles downstream.

As wireless communication technology has advanced in recent years, a few studies have focused on developing more comprehensive traffic signal control systems, especially using Connected Vehicle (CV) technology [8]. Some of them formulated the problem into a nonlinear constrained programming formulation [9], which potentially obstructs the online implementation of the algorithm. Others used aggregated performance measures (e.g., platoon [10] or passing rate [11]) for computational tractability, without taking full advantage of each individual vehicle's information (e.g., speed trajectory, vehicle type and turning movement) available via vehicular communications. A very recent study developed a multi-agent system (MAS) based traffic signal priority control algorithm using CV technology [12], where the information of individual vehicle type (freight vehicles in particular) is utilized to activate the optimization of traffic signal timings for environmental sustainability. However, due to computational costs, the phase sequence was fixed for the sake of real-time implementation. It should be pointed out, despite these efforts, a computationally attractive as well as structurally flexible online adaptive traffic signal control (ATSC) strategy is still needed under the Connected Vehicle environment.

Although DSRC was originally developed to support safety applications, both mobility and environmental applications can also benefit greatly from using DSRC. In fact, DSRC provides both the foundation and framework for nearly all ITS applications, and additional message formats are

being designed specifically for further enabling ITS applications. The ITS applications presented in chapters 3 and 4 make use of DSRC within the context of V2I communications near traffic intersections.

2.2 Conventional Traffic Signal Control

Conventional traffic signal control for 4-leg intersections uses the standard National Electrical Manufacturers Association (NEMA [13]) signal phases, as shown in Fig. 1 below. For each leg of the intersection, there are three movements: a left-turn movement, a through movement, and a right-turn movement. Typically, the right-turn movement for a given intersection leg is permitted to be concurrent with the intersection leg's through movement. Therefore, there are a total of eight signalized phases at a conventional 4-leg intersection. The 8 phases are divided into main street and side street phases, as indicated in the right-side portion of Fig. 1. The phases are further divided into 2 rings. Both rings, {1, 2, 3, 4}, and {5, 6, 7, 8}, consist of self-conflicting phases. Two phases are non-conflicting if they are on the same side of the barrier and in different rings. For example, phase 1 may be active with either phase 5 or phase 6. Each column shown in the phase table on the right-side portion of Fig. 1 represents a dual-ring signal phase. A typical cycle consists of serving the 8 individual phases with 4 dual-ring phases. The main street movements are usually served before the side street movements and are given a larger "split" of the total cycle length time than the side street movements. In addition, the left-turn movements on each side of the barrier usually precede the through and right-turn movements.
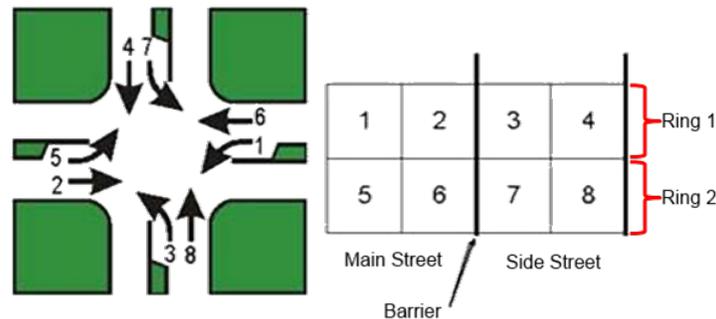

Fig. 1: NEMA Dual-Ring Phasing Diagram, adapted from [14]

Traffic signals may be controlled based on either fixed signal timing or actuated/adaptive signal control timing. Fixed signal timing uses fixed cycle lengths and fixed signal splits based on historical traffic data and field observations. Actuated/adaptive signal control timing makes use of sensors such as inductive loop detectors (ILDs), video cameras, or radar/LiDAR sensors to modify signal timing based on the real-time arrivals of vehicles. The term "actuation" refers to the activation of one or more sensors, whereas "adaptive" is used to indicate that the signal timing is being modified based on the detection of vehicles. There are a number of adaptive signal control optimization systems that have been deployed including OPAC, PRODYN, RHODES, SCAT, and SCOOT [15]. Additional signal timing optimization methodologies include TRANSYT [16], PASSER II, MAXBAND, and MULTIBAND [17]. The primary disadvantage of each of the aforementioned systems and methodologies is that they rely on point detection and consequently may inaccurately estimate state information.

3. Isolated Intersection Connected Vehicle Signal Optimization

3.1 Application Description

Conventional adaptive signal control strategies make use of point detection sensors such as inductive loop detectors (ILDs), video sensors, or radar/LiDAR sensors to adjust the signal timing based on the limited available knowledge of incoming traffic. Each of the aforementioned sensors has one or more significant drawbacks such as accuracy, occlusion, and degraded performance due to adverse lighting or weather conditions. Each of the traditional sensor drawbacks is circumvented with the use of wireless CV technology. The following section describes an adaptive signal control optimization strategy based on using CV technology to build a complete and accurate picture of real-time traffic conditions near an arterial intersection.

3.1.1 System Introduction

Considering traffic at an intersection to be a multi-agent system (MAS), the signal phase and timing may be controlled to improve overall traffic efficiency. A multi-agent system is a computerized system composed of multiple intelligent agents interacting within an environment. At a given intersection, two types of agents may be considered: 1) Vehicle Agents (VA), and an 2) Intersection Management Agent (IMA). The role of the VA is defined as including communicating ego information to the IMA. The role of the IMA is defined as including communicating with all VA's within a communication radius, and determining the optimal signal timing. The overall system architecture is presented in the following subsection. Next, an extension of the dual-ring traffic controller is introduced, followed by a description of the signal timing optimization method utilized.

3.1.2 System Architecture

As shown in Fig. 2, the system consists of multiple vehicle agents interacting with a single intersection management agent. Each IMA is intended to control a single intersection. Due to the nature of adaptive signal control, the following strategy is readily extended to multiple intersections and corridors. Alternative implementations may also include VAs communicating with each other.
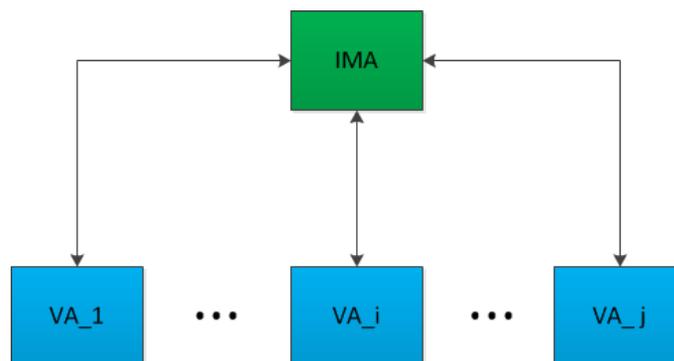

Fig. 2: CV MAS Level 0 Diagram: Top-level System Architecture

The intersection management agent controls the traffic signal lights based on received information from all of the VAs within communication range of the intersection. As indicated in Fig. 3, the IMA makes use of several signal timing constraints to determine when the signal timing

needs to be changed. These constraints include the minimum green time, maximum green time, yellow time, as well as the "all-red" duration. If none of these constraints are in effect, then the IMA re-evaluates the traffic environment every one second in order to determine if a change in signal timing is necessary for optimizing the user-defined Measure of Effectiveness (MOE). Among others, MOEs may include queue length, idling time, energy consumption, or number of stops. Based on the selected MOE, a VA may need to predict certain information in order to provide the IMA with input. For example, if the selected MOE is travel delay, then VAs need to predict Time-Of-Arrival (TOA) based on proposed Signal Phase and Timing (SPaT) plans. The VA actions are detailed in Fig. 4. If a VA is within communication range of the intersection, it receives the stop bar location from the IMA. Using the stop bar location, if a VA is approaching the traffic signal, it then sends the necessary ego information to the IMA (based on the selected system-wide MOE).
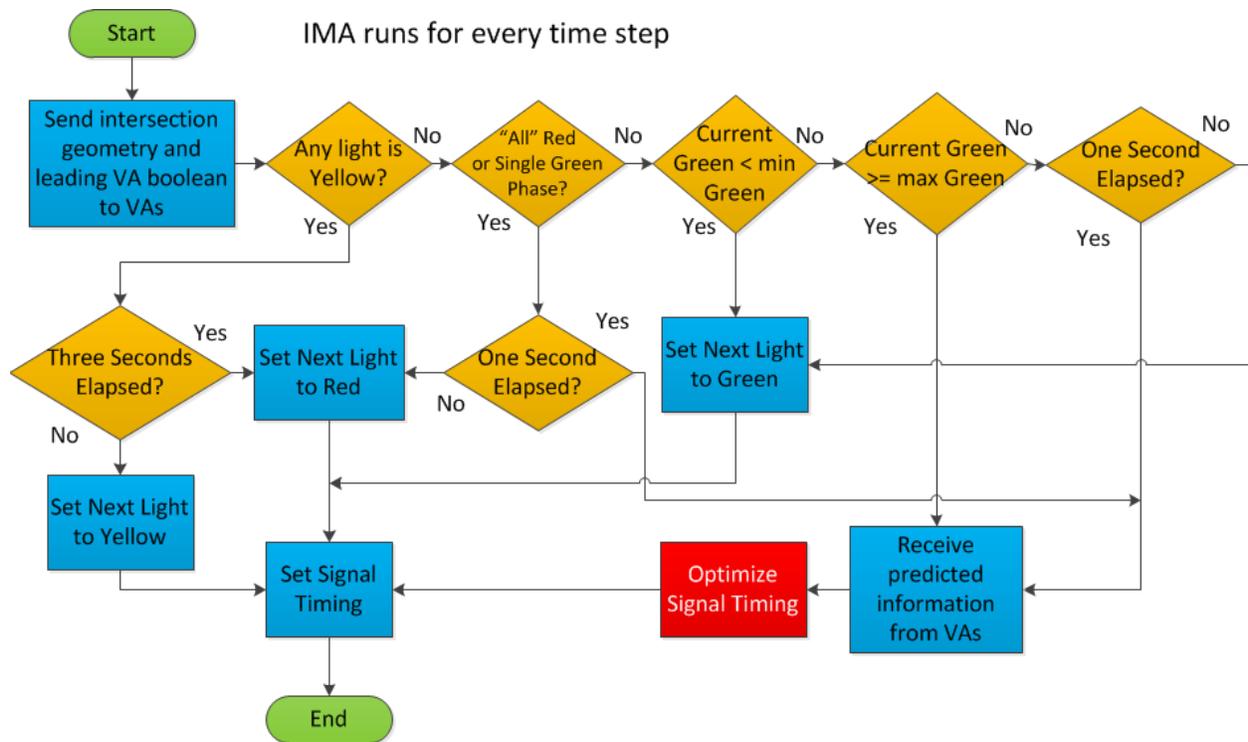

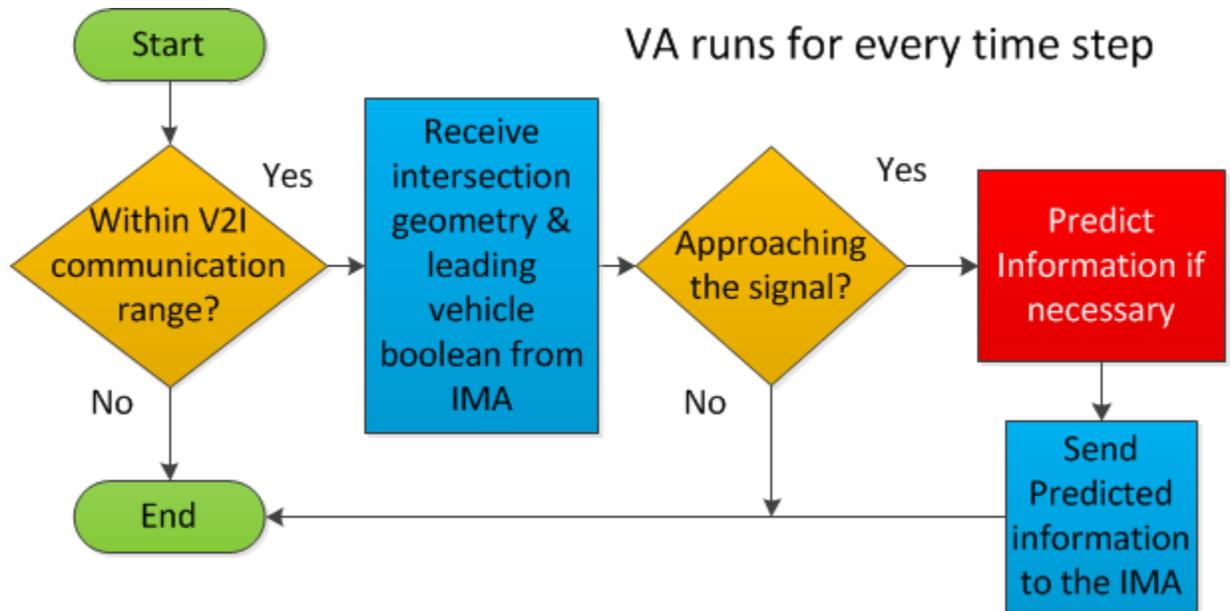Fig. 3: CV MAS Level 1 Diagram: Intersection Management Agent Flow Chart

Fig. 4: CV MAS Level 1 Diagram: Vehicle Agent Flow Chart

3.1.3 Fixed & Flexible Traffic Light State Machines

Perhaps the most common traffic controller used in the United States is the dual-ring National Electrical Manufacturing Association (NEMA [13]) controller. Fig. 5 includes the dual-ring controller and the corresponding NEMA signal phase diagram. The two "rings" correspond to two sets of self-conflicting phases, phases {1, 2, 3, 4} belonging to "Ring 1" and phases {5, 6, 7, 8} belonging to "Ring 2." At any given time instant, two signal phases are active, one from each ring. The two rings operate independently, with the restriction that the selected phases must be on the same side of the barrier (e.g. phases 2 and 7 cannot be active simultaneously). Main street phases are normally numbered as {1, 2, 5, 6}, while side street phases are typically numbered as {3, 4, 7, 8}. A typical background cycle consists of a fixed pairing and sequence of phases, with the main street movements being served prior to the side street movements. For a standard 4-leg intersection, there are four green phases per cycle, separated by appropriate yellow and red phases. Fixed signal timing uses pre-determined durations (splits) for each of the four green phases and uses the fixed sequence and combination of phases prescribed in Fig. 5. As shown in Fig. 5, signal operation starts with phases 1 and 5, followed by 2 and 6, 3 and 7, and 4 and 8, before repeating.
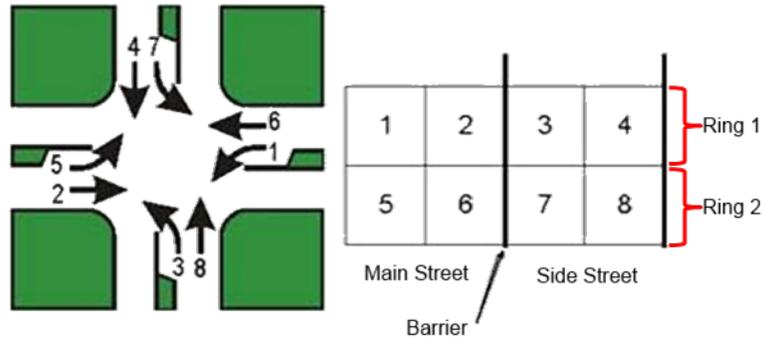
Fig. 5: Signal Phase Diagram & Dual-Ring Controller, adapted from [14]

To further illustrate the limitations of the fixed signal timing interpretation of the dual-ring controller, the fixed sequence of traffic signals may be represented using a finite state machine, as shown in Fig. 6. Including yellow and red phases, there are a total of 9 unique states, with the "All" red phase repeated in the transition between every phase. Previous work was based on using the fixed sequence of traffic signals as prescribed by the dual-ring controller, and focused on optimizing the duration of each of the green splits [12]. However, a fully adaptive signal control paradigm should also consider optimizing phase sequence in addition to phase duration. Moreover, it is not necessary to have a strict coupling of phases such as 1 and 5, and 2 and 6. In fact, phase 1 may operate with either phase 5 or 6. By permitting the rings to operate independently, the dual-ring controller may be represented with a more advanced and flexible finite state machine, as shown in Fig. 7. The red cylinder, labeled as the "All Red" state, represents the barrier, as well as the only link, between the main street and side street phases. There are four "green" states on each side of the barrier, for a total of eight "green" states. The main street half of the diagram in Fig. 7 is shown in Fig. 8. The side street half of the diagram in Fig. 7 is nearly identical to the main street half, and is shown in Fig. 9. "Green" colored states occur where two green phases are active. "Yellow" colored states occur where at least one signal phase is yellow. Finally, "Red" colored states occur where all traffic lights are red, or if all but one signal phase is red.
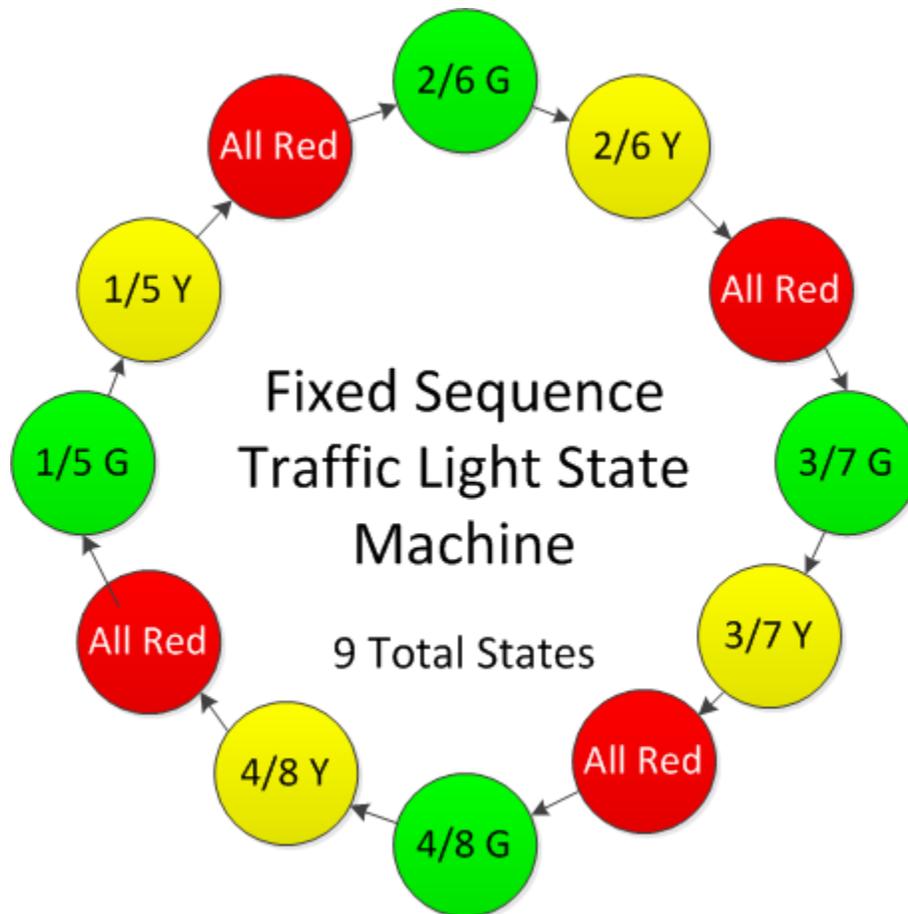
Fig. 6: Fixed Sequence & Coupled Phase Dual-Ring Controller, Finite State Machine Representation
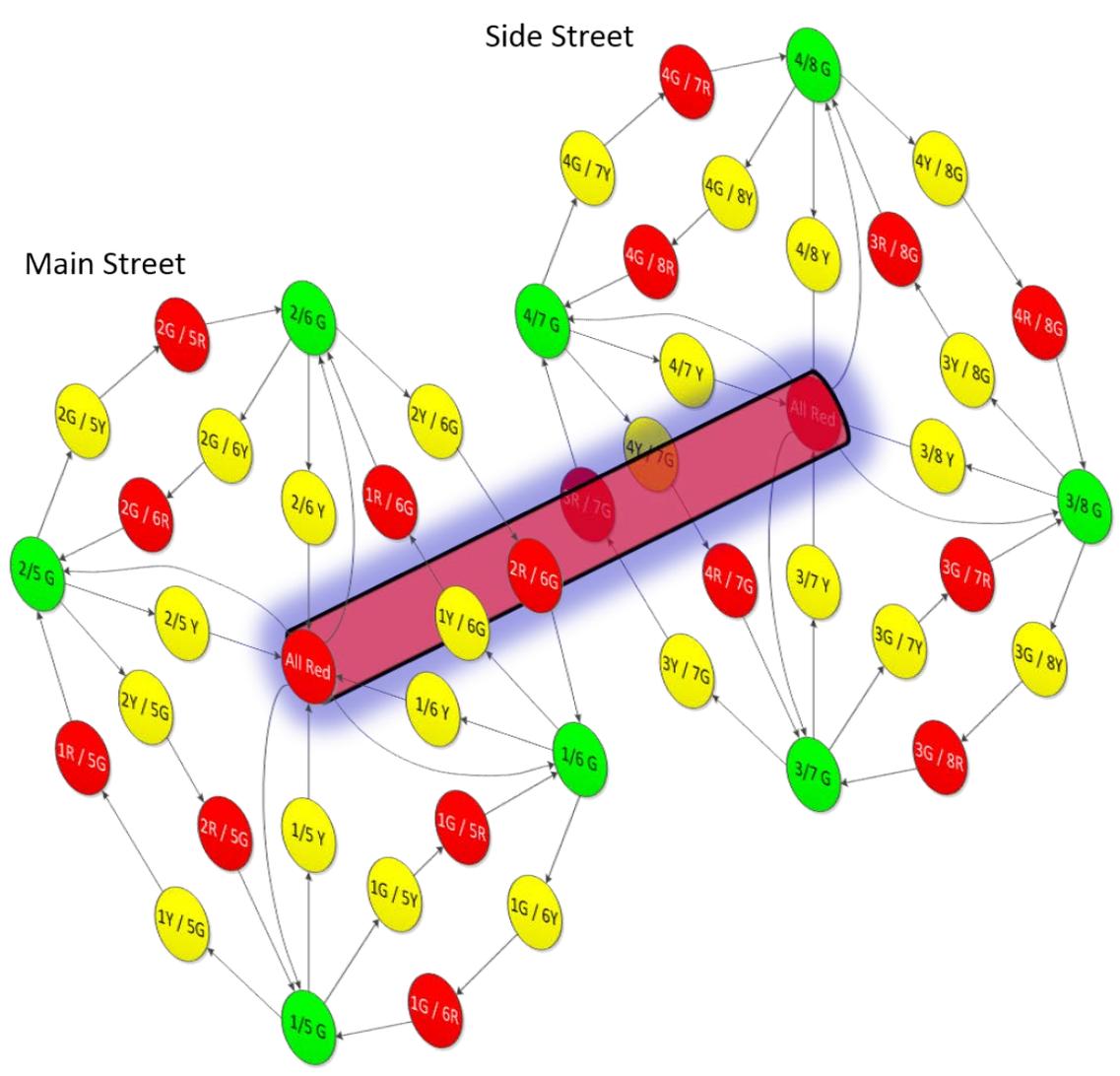
Fig. 7: Flexible Dual-Ring Controller, Finite State Machine Representation

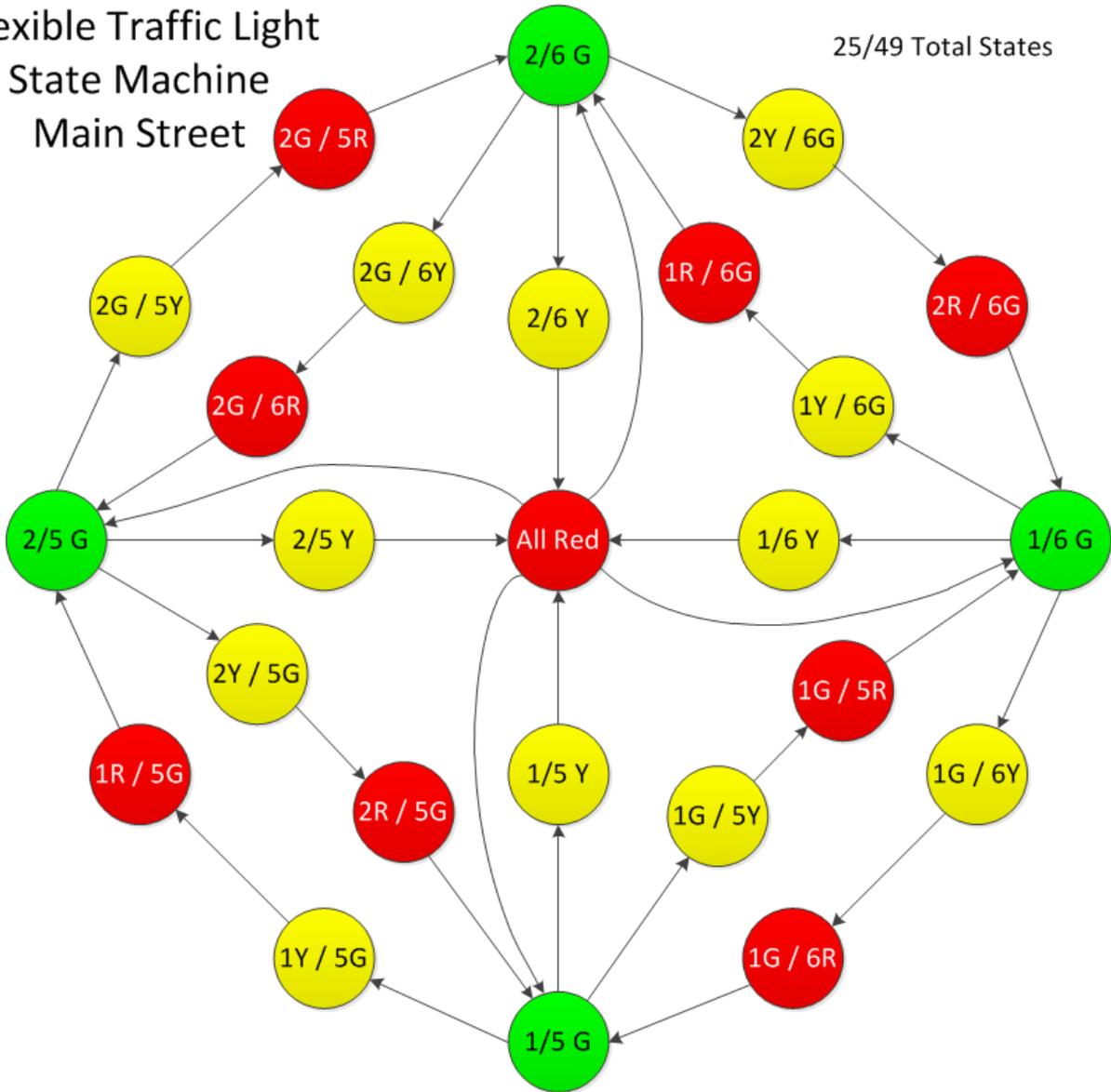Fig. 8: Main street portion of Flexible Dual-Ring Controller, Finite State Machine Representation
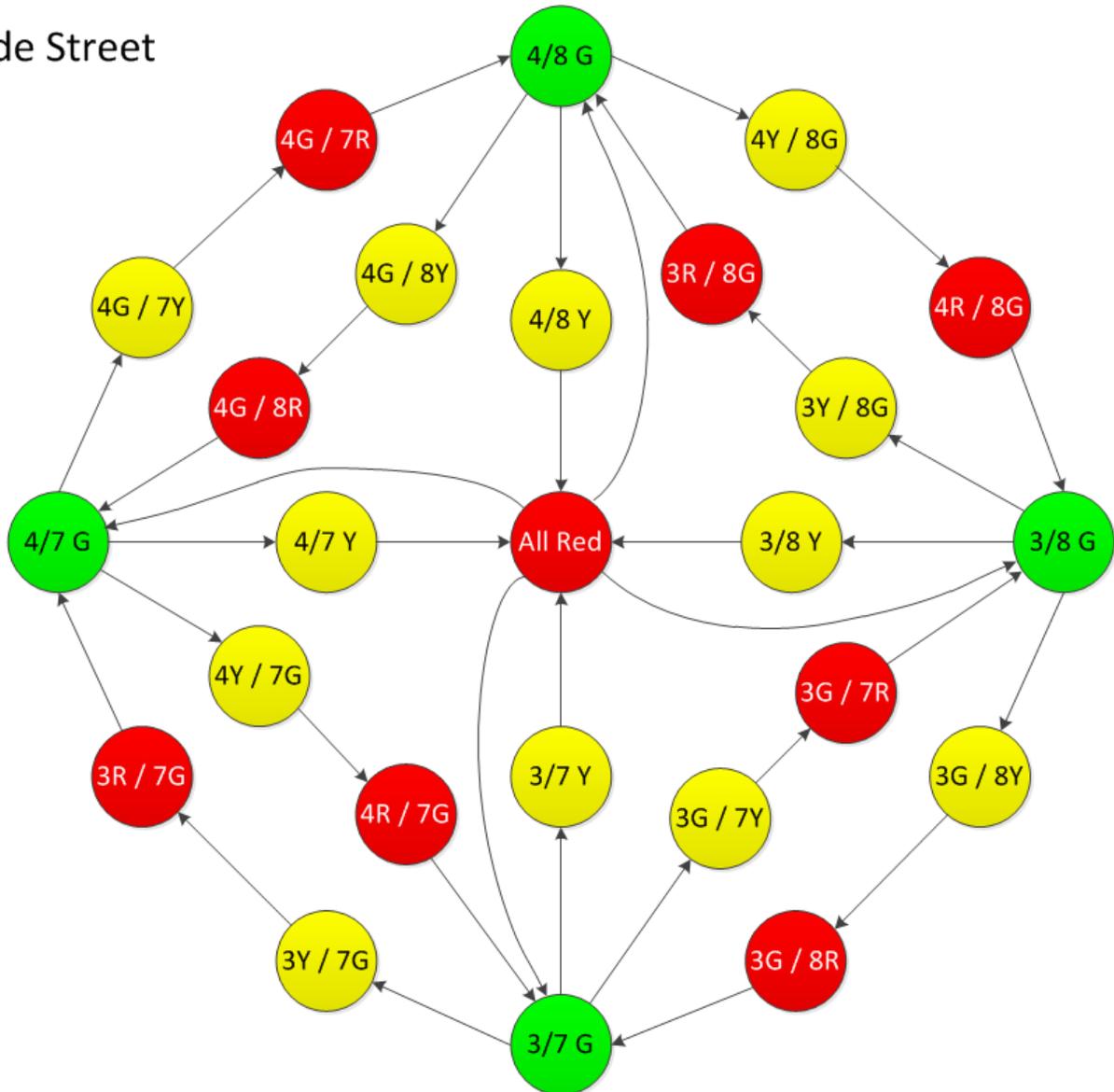
Fig. 9: Side street portion of Flexible Dual-Ring Controller, Finite State Machine Representation

The total of 49 states allow for a variety of signal strategies to be implemented by the IMA, including "green extension," "early green," "phase insertion," and "phase rotation." Furthermore, the diagram shown in Fig. 7 also indicates state transition information. At any given state, the set of possible next states is fully specified. In summary, the proposed flexible traffic light state machine provides a convenient framework for visualizing adaptive signal control and providing state transition information to the IMA.

3.1.4 Signal Timing Optimization and MOE Selection

Using the flexible traffic light state machine presented in the previous section, signal phase duration and sequence may be optimized by the IMA to implement any specified MOE. Although MOEs may be easily compared in a simulation environment, additional factors must be

considered for field deployment and system structure. Additional factors for consideration include the accuracy, accessibility, and privacy of information, computational complexity, and where the MOE falls on the scale of "proactiveness" and "reactiveness". The accuracy of information is of vital importance for optimizing signal timing. Some MOEs, such as the travel time MOE, make use of predicted information to determine how overall travel times of individual vehicles might be impacted by potential signal phasing strategies. Any discrepancies between the predicted information and the eventual course or timing of events lead to sub-optimal performance of the signal optimizer. The accessibility, or ease of access, of information is an important consideration for physically implemented CV environment systems. Accessibility poses the practical question of whether a connected vehicle can obtain, package, and transmit the desired information in a timely manner. An example of an MOE with potentially poor accessibility is an MOE that relies on real-time vehicle emissions information. An issue which is increasingly gaining attention is the privacy and security of information in CV environments. Since vehicles would be potentially transmitting detailed state information, the concern is that a connected vehicle could be tracked, or even worse hacked. The issue of computational complexity restricts MOE selection to MOEs that are mathematically tractable, and can be operated in a physical system in real-time. Finally, the consideration of proactivity versus reactivity is a system design issue. Reactivity is defined as an intersection merely responding to existing state information. Proactivity is defined as utilizing existing state information to predict future state information as an input into the signal optimization. An entirely reactive MOE has the benefit of using accurate information, but may fall behind in terms of providing the appropriate signal timing phases at the optimal time. In contrast, a completely proactive MOE has the benefit of staying ahead of current traffic conditions, but may be compromised by inaccurate predictions. As a result, an effective MOE strikes a balance on the scale of proactiveness and reactiveness.

Based on the above considerations, a number of MOEs including travel time, current delay, and queue length, and their variants, were explored in the process of selecting an appropriate MOE for a CV environment. Ultimately, a variation of queue length was selected as the most appropriate MOE for real-time signal optimization in a CV environment. The MOE of queue length satisfies all of the considerations listed in the preceding paragraph. For example, the queue length MOE is based on obtaining information on whether a vehicle is within range of an intersection and whether its speed is less than a maximum speed threshold. As a result, the queue length MOE relies on information that is 100% accurate, (whether a vehicle is in range of an intersection), and information that is easily accessible by vehicles (vehicle speed). Another advantage of the queue length MOE is that vehicles are able to maintain privacy because they do not need to be tracked by the intersection. In terms of computational complexity, the queue length MOE is one of the simplest and most attractive MOEs for use in real-time signal optimization. Finally, on the scale of proactiveness and reactiveness, queue length generally falls closer to the reactive portion of the scale. However, increasing the maximum speed threshold under which vehicles are defined as being queued can move the queue length MOE closer to the center of the scale. For example, in a purely reactive queue length scheme, the maximum speed under which vehicles are queued is set to 0 mph, and only vehicles completely at rest will be served by a given signal phase. In contrast, a partially proactive queue length scheme considers

vehicles which are about to stop as also being queued, which removes the constraint that vehicles must be completely stopped before being served by the intersection. Consequently, based on the advantages listed above, the results presented in subsequent sections utilize queue length as the MOE to evaluate the effectiveness of the proposed agent-based online adaptive signal control strategy.

Numerous variations of queue length optimization exist; therefore, a description of the exact queue length optimizer implemented follows, as shown in Fig. 10. Queued vehicles were defined as vehicles within the communication radius of the IMA which had a velocity less than a user-defined threshold (e.g., 10 mph), and were approaching the intersection. The diagram in Fig. 10 corresponds to the red block presented in Fig. 3.
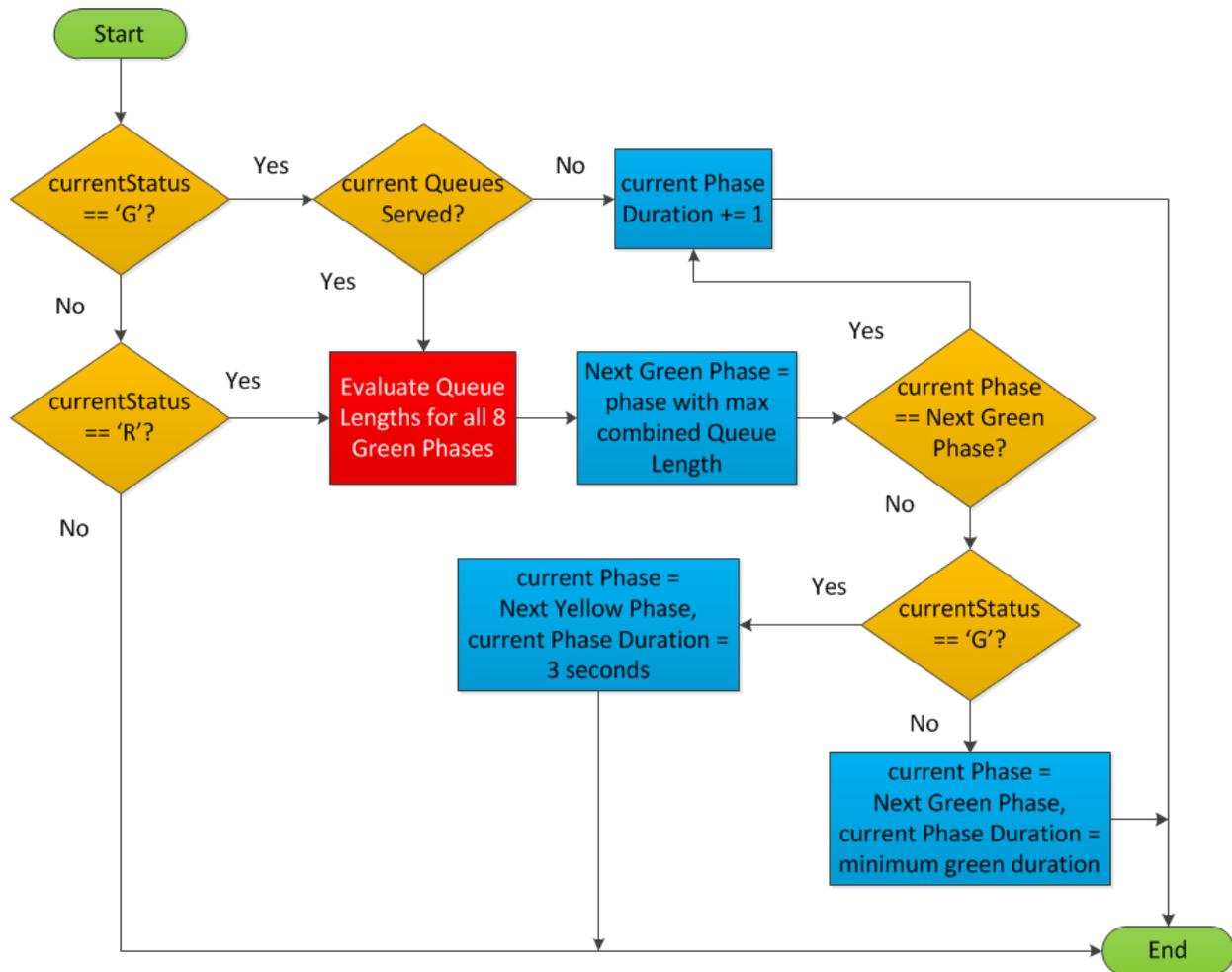
Fig. 10: CV MAS Level 2 Diagram: Queue Length Signal Optimizer

The essential idea of the proposed queue length optimizer is to maximize the number of vehicles that are being served with a green light at the intersection. In order to reduce freight vehicle emissions, freight vehicles may be considered as the equivalent of several light-duty vehicles in terms of queue length. Recall from the IMA flow chart presented in Fig. 3, that the signal

optimizer is only called after a green phase has exceeded its minimum green allotment, or if the "All Red" state is expired. These two conditions are denoted in Fig. 10 as the current state of the traffic light being either "G" or "R," respectively.

If the state is "R," the optimizer evaluates all eight possible green states to find the state with the maximum combined queue length across all lanes of the selected movements. Once the optimal next state is calculated, the current phase is set to the selected green state, and is assigned the minimum green duration. In addition, all vehicles on any lane of the selected phases are internally marked as being currently served. The rationale behind keeping track of which vehicles are currently served is to allow the queues to fully discharge and avoid the undesirable "partial queue discharge" effect. The "partial queue discharge" effect occurs when a signal controller switches phases because the queue lengths on the currently served phases decrease (due to being currently served) to the point that a different phase combination has a larger combined queue length. The effect is undesirable because it leads to multiple stops for vehicles being served, and increases the loss time due to frequently switching phases.
After transitioning from a red colored state (Fig. 7), the state becomes "G," and at the end of the minimum green duration, the IMA checks if all of the vehicles originally marked as being currently served have passed the stop bar. If not, the current green phase is repeatedly extended in one second increments until all of the marked vehicles have passed into the intersection. The proposed approach has the advantage of being able to switch to a green phase without having to predetermine its duration. Since additional vehicles may enter the currently served phase during the discharge of the marked queues, the possibility of remaining on the same green phase after the current queues have been served is permitted.

One issue that arises with the use of MOEs such as queue length for signal optimization is "green starvation." Green starvation occurs when certain approaches to an intersection consistently have lower traffic volumes than other approaches. For example, if there is only one vehicle turning left from a minor street onto a major street, the traffic signal may prefer to keep serving the busier major street instead of switching to the minor street. In this case, although the IMA would be optimizing overall system performance by ignoring the single vehicle, the notion of fairness must be introduced. A single vehicle should not have to wait several minutes in order to be served by the intersection. One solution to the problem of green starvation is to modify the queue length MOE to incorporate information about the time elapsed since a particular signal phase was last served. If the time elapsed since a particular signal phase was last served is relatively high, then the queue length on that phase is weighted higher than the queue length on a signal phases that was more recently served. Essentially, the queue length is multiplied by "aging" factors. The relationship between the time elapsed since a signal phase was last served and the value of the multiplicative aging factors can be adjusted based on individual localities needs. For the results shown in the following sections, the relationship between the time elapsed since a signal phase was last served and the value of the multiplicative aging factor was set to be a quadratic equation fitting the points (0, 1), (30, 2), and (120, 10), where x is the input (elapsed time in seconds), and y is the output (aging factor value). The first point corresponds to the queue length remaining unmodified if the signal phase was just served. The second point corresponds to the queue length being weighted twice as high as normal if half a minute has

elapsed since the signal phase was last served. Finally, the third point corresponds to the queue length being weighted 10 times higher than normal if a full two minutes has elapsed since the signal phase was last served. A plot of the quadratic equation is shown in Fig. 11 below.
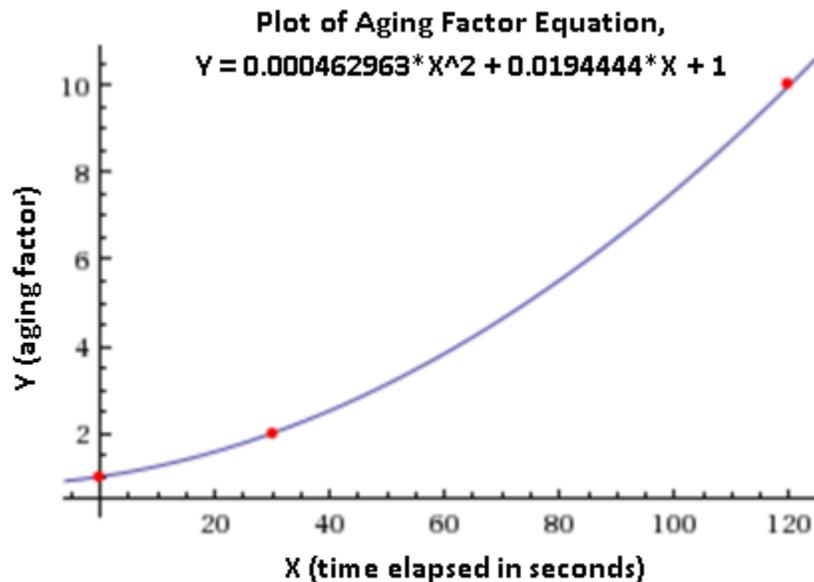

Fig. 11: Plot of Quadratic Aging Factor Equation

3.2 Simulation Setup

In order to implement the adaptive CV signal optimization strategy in simulation, PARAMICS 6.9.3 was selected [18]. In addition, EPA's MOVES software [19] was integrated in order to provide information on the environmental performance metrics, including energy usage. The overall simulation software system diagram is shown in Fig. 12 below. The adaptive CV signal optimization strategy was tested in comparison to several baseline strategies for various sensitivity analyses. The first baseline simulated was an intersection with fixed phase signal timing where the cycle length was fixed at 120 seconds. The second baseline simulated used a cycle length calculated using the unmodified Webster's formula for cycle length. The unmodified equation for Webster's cycle length, C, is $C = (1.5 * L + 5)/(1 - CS/S)$, where L is the loss time in the cycle due to the duration of yellow and red signal phases, where CS is the sum of the critical lane volumes over every signal phase for the intersection, and where S is the saturation flow rate. Once the cycle length is determined, the signal splits are determined based on the ratios of critical volumes for each phase. A third baseline was also implemented for the demand profile sensitivity analysis, where cycle length is calculated using the HCM method [20]. In terms of general simulation parameters, the speed limit for each intersection was set at 45 mph. Each simulation run was conducted for 1 hour, with additional time to permit all vehicles to exit the simulation.
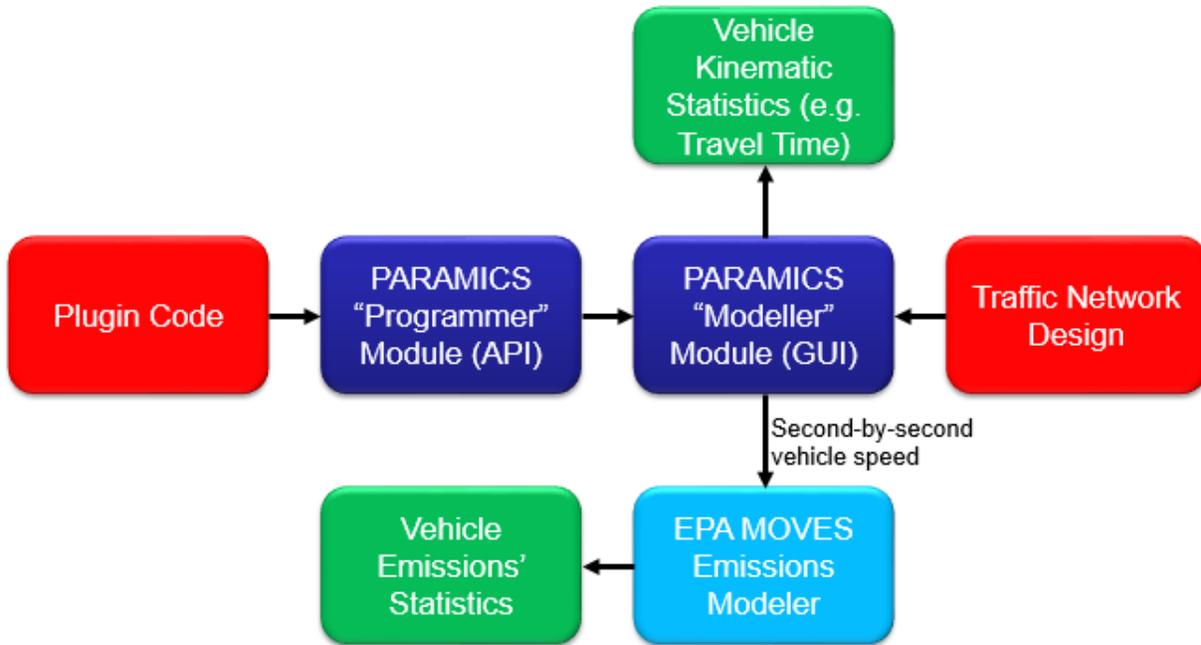
Fig. 12: Microscopic Traffic Simulation System Diagram

3.3 PARAMICS Network Description

The isolated intersection used to evaluate the adaptive CV signal optimizer and the baseline signal control strategies is shown in Fig. 13 below. The adaptive signal control version of the intersection used PARAMICS movement priorities in order to fully control the intersection movements. A second version of the intersection for testing the baseline signal control strategies used PARAMICS built-in signal control module. Nevertheless, the physical layout of the intersection remained identical for both versions of the network.   The intersections were designed to have 4 approaches, with 3 lanes each, plus a left-turn bay of 500 feet. The overall dimensions of the intersection were 2414 feet by 2414 feet. The turning movements for the lanes are shown in Fig. 14 below. From left to right, the left-most lane was set as an exclusive left-turn lane, the middle two lanes were set as through-only lanes, and the right-most lane was set as a shared through and right-turn lane with a right-turn on red policy. As shown in the upper right portion of Fig. 13, a GUI was developed to indicate which signal phase was active, and to display the queue lengths of each phase in real-time. Every signal phase starts at a minimum of 8 seconds, and is extended as necessary to fully clear the queue of vehicles being served. The upper left portion of Fig. 13 includes a red box which indicates the current maximum length phase during the simulation.
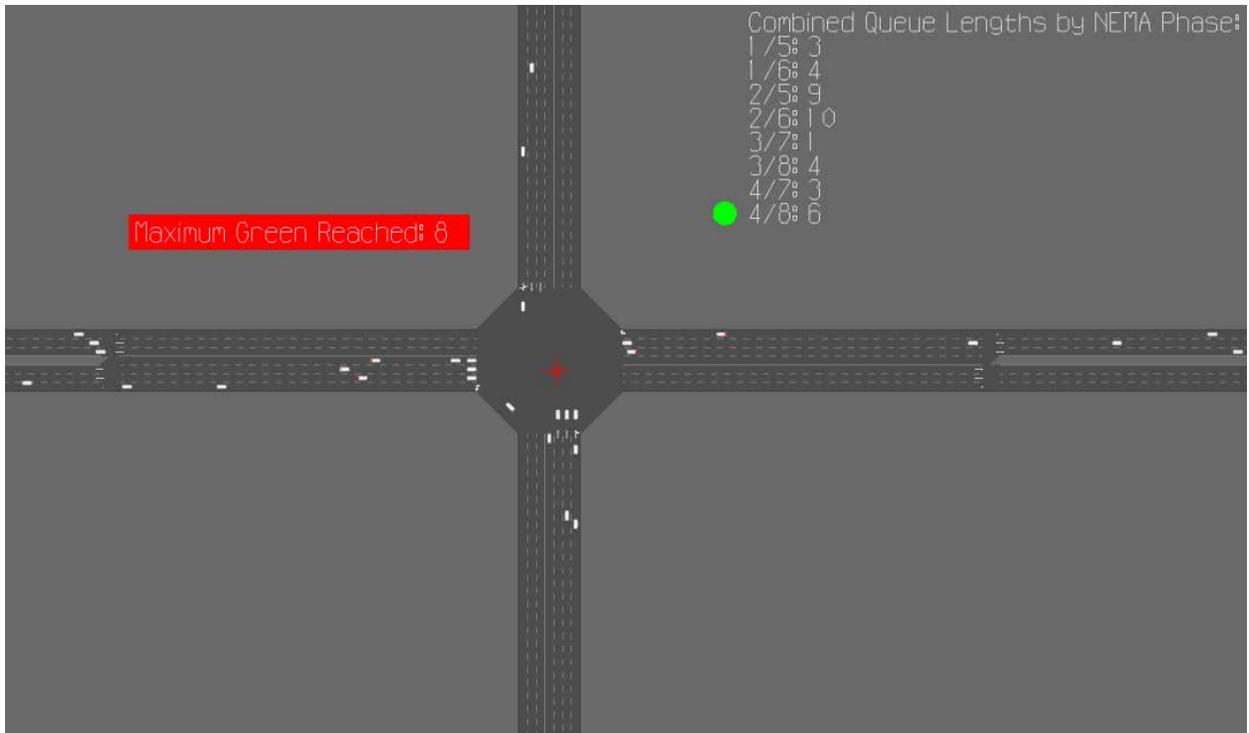
Fig. 13: Isolated Intersection PARAMICS Network
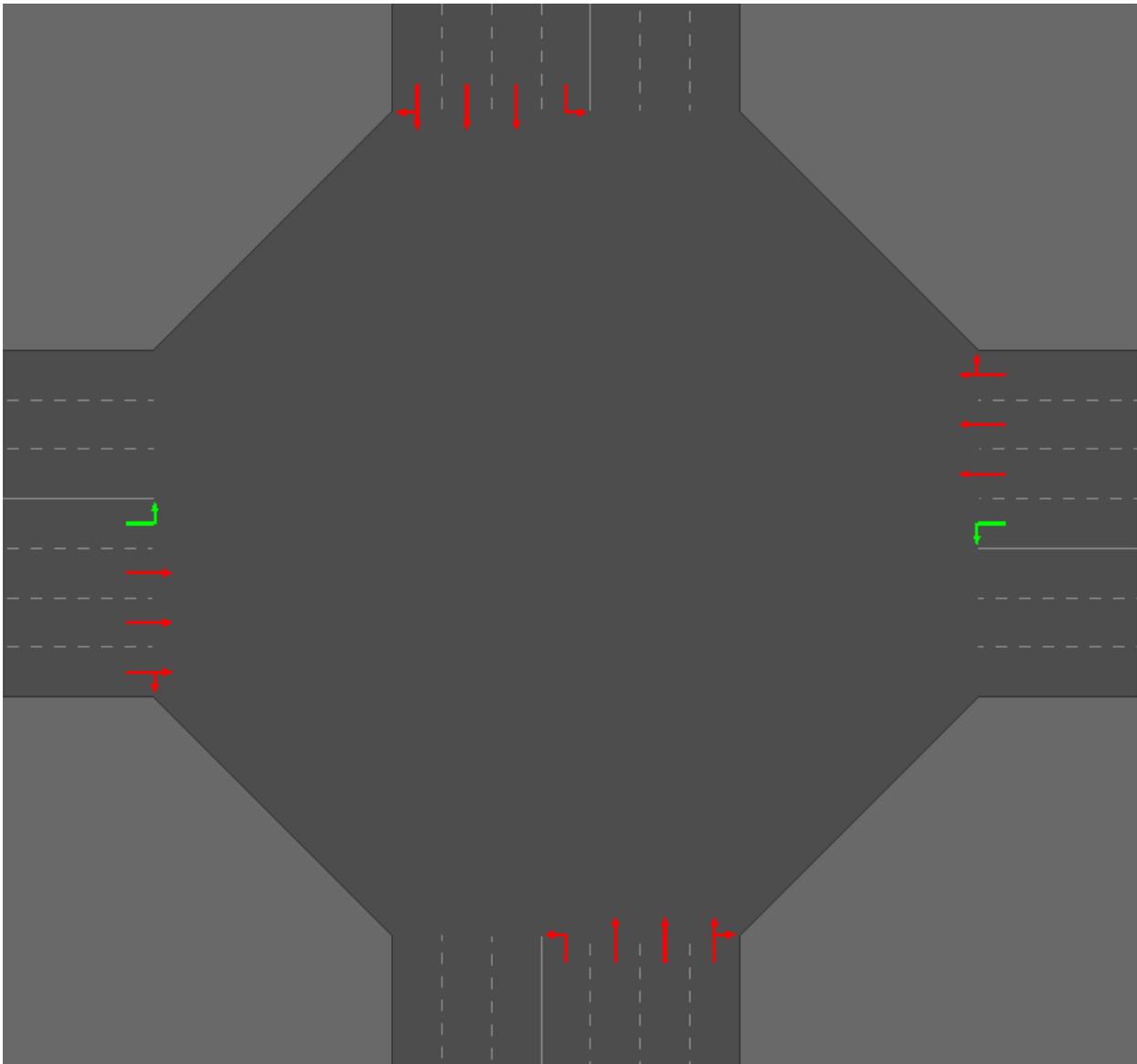
Fig. 14: Turning Movements for Isolated Intersection

3.4 Volume Sensitivity Analysis

For the volume sensitivity analysis, a series of traffic volumes ranging from 1000 vehicle per hour to 6000 vehicles per hour in 500 vehicles per hour increments was tested. The overall traffic on the major street was set to be 50% higher than the traffic on the minor street, and the turning ratios for left-turn movement, through movement, and right-turn movements was set to 20%, 70%, and 10%, respectively. In addition, a constant demand profile over the course of the one-hour simulation was used.

3.4.1 Connected Vehicle Queue Length Signal Optimization versus Fixed Phase Signal Timing

The CV queue length optimizer is given no information regarding incoming traffic. In contrast, the signal splits for the fixed phase signal timing intersection are determined based on complete knowledge of the origins and destinations of the incoming traffic. The assumption of *a priori* information being available to the fixed phase signal timing intersection is equivalent to the signal timing being perfectly tuned. The results for the CV queue length signal optimizer relative to fixed phase signal timing are shown in Figs. 15-19 and Tables I-III. The travel time savings are highest at low traffic volumes, and gradually decrease as traffic volume is increased, until the time savings are erased at 6000 vehicles per hour. An identical trend may be observed in terms of energy saved by using CV queue length signal optimization instead of fixed phase signal timing. The energy benefits are highest at low traffic volumes, and decrease as the traffic volume increases. The emissions savings ranged primarily from -5% to 15%, with the greatest savings occurring at low traffic volumes. The emissions savings are positive at the lower volumes because the intersection is able to more quickly respond to incoming vehicles as opposed to vehicles which may have to wait at a fixed phase signal the better part of a 120 second cycle in order to be served regardless of the absence of vehicles on other signal phases. The emissions savings are slightly negative at high traffic volumes due to an increase in the number of vehicle stops. The increase in the number of vehicle stops is due to the intersection beginning to reach its capacity.

Due to the addition of the dedicated left-turn bay, the capacity of the intersection is around 6500 vehicles per hour. The results indicate at near saturated conditions, adaptive signal control does not provide additional benefits over fixed phase signal timing. Generally, fixed phase signal timing is considered a relatively weak baseline; however, under near saturated and saturated conditions, fixed phase signal timing performs better than adaptive signal control strategies.

Fig. 15: Average Travel Time Comparison of CV Queue Length Signal Optimization and Fixed Phase Signal Timing for an Isolated Intersection

Fig. 16: Average Travel Time Percent Savings of CV Queue Length Signal Optimization over Fixed Phase Signal Timing on an Isolated Intersection
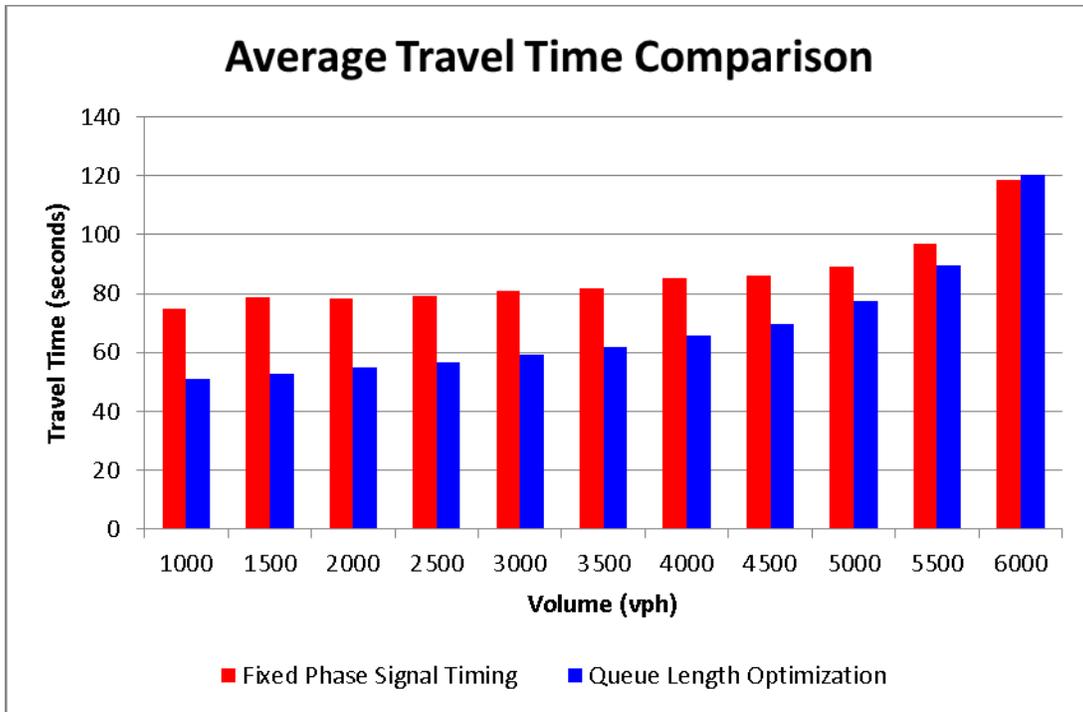
Fig. 17: Average Energy Comparison Of CV Queue Length Signal Optimization and Fixed Phase Signal Timing for an Isolated Intersection
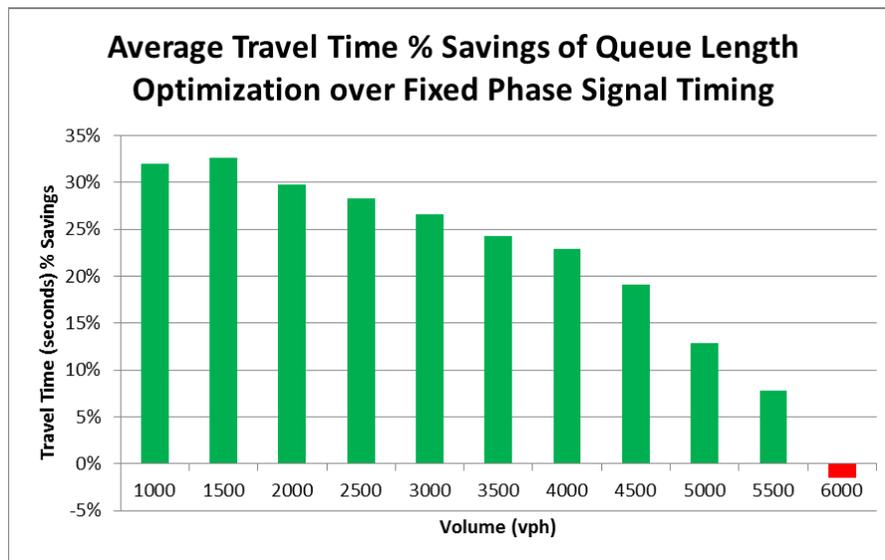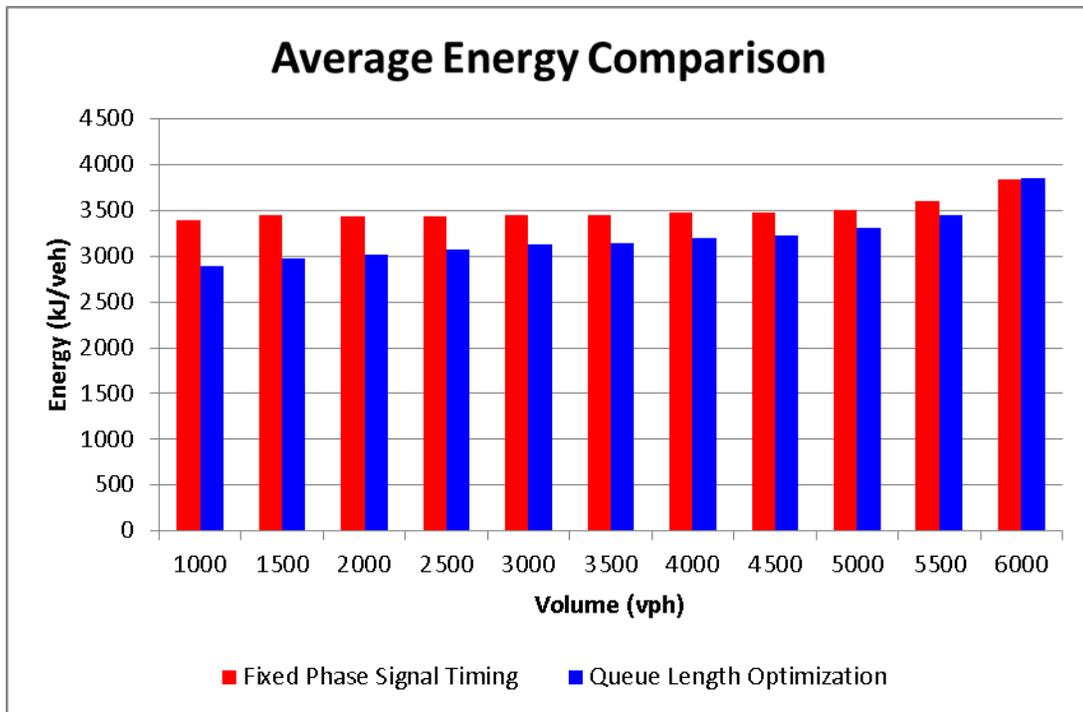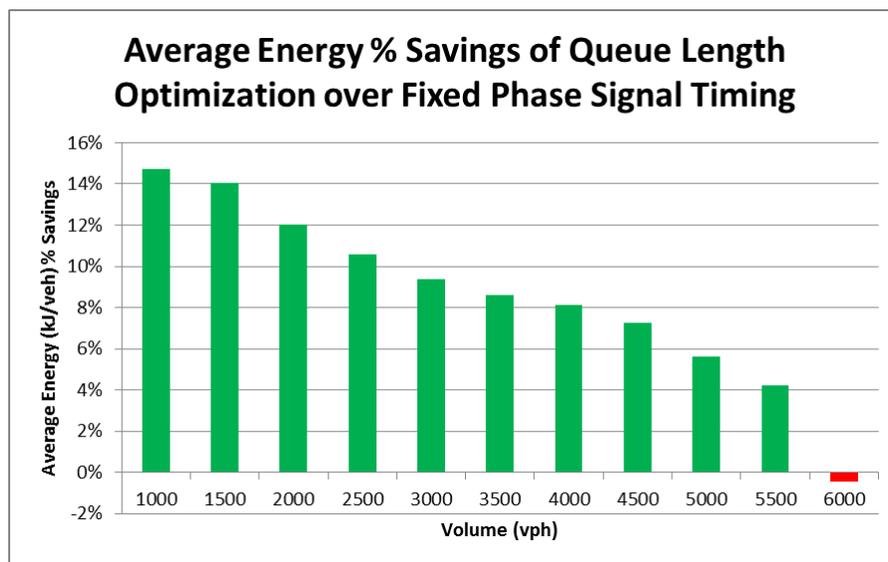

Fig. 18: Average Energy Percent Savings of CV Queue Length Signal Optimization over Fixed Phase Signal Timing on an Isolated Intersection
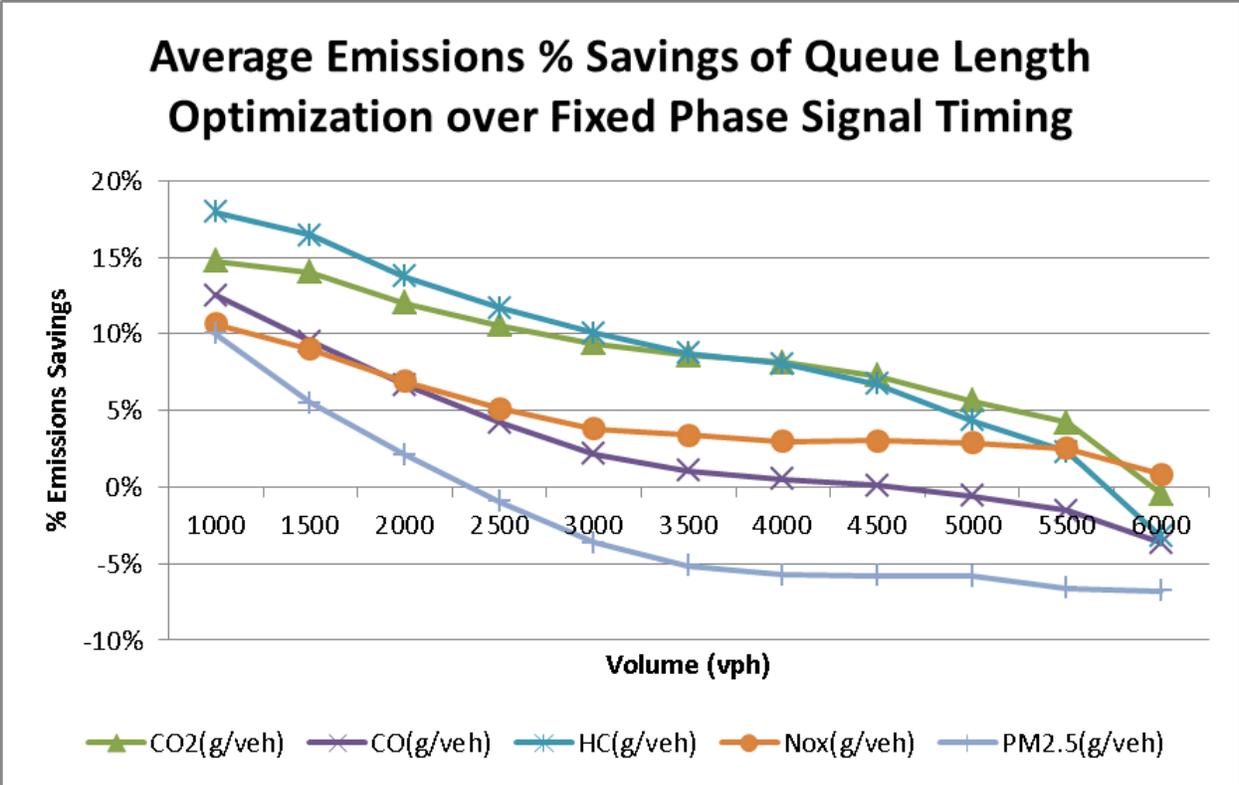
Fig. 19: Average Emissions Percent Savings of CV Queue Length Signal Optimization over Fixed Phase Signal Timing on an Isolated Intersection

Table I: Fixed Phase Signal Timing, Traffic Volume Sensitivity Analysis Results

Volume (vphpi)	Energy (kJ/veh)	CO2 (g/veh)	CO (g/veh)	HC (g/veh)	NOx (g/veh)	PM2.5 (g/veh)	VHT (s/veh)
1000	3388.3116	243.5169	5.3228	0.1662	0.5759	0.0389	74.8485
1500	3455.2288	248.3262	5.3119	0.1689	0.5814	0.0382	78.5087
2000	3430.3610	246.5389	5.2031	0.1666	0.5747	0.0371	78.2152
2500	3436.9265	247.0108	5.1667	0.1665	0.5732	0.0367	78.9594
3000	3448.2000	247.8210	5.0976	0.1666	0.5705	0.0358	80.8024
3500	3443.3450	247.4721	5.0291	0.1660	0.5660	0.0350	81.7712
4000	3483.9148	250.3878	5.0226	0.1682	0.5661	0.0346	85.2737
4500	3482.0136	250.2512	4.9640	0.1678	0.5625	0.0339	86.2439
5000	3506.8703	252.0376	4.9296	0.1691	0.5606	0.0333	89.0625
5500	3597.5330	258.5535	4.9426	0.1747	0.5613	0.0327	97.0571
6000	3840.3389	276.0037	5.0622	0.1894	0.5704	0.0323	118.7739

Table II: CV Queue Length Signal Optimization, Traffic Volume Sensitivity Analysis Results

Volume (vphpi)	Energy (kJ/veh)	CO2 (g/veh)	CO (g/veh)	HC (g/veh)	NOx (g/veh)	PM2.5 (g/veh)	VHT (s/veh)
1000	2888.9053	207.6249	4.6571	0.1364	0.5145	0.0350	50.8897
1500	2970.3667	213.4795	4.8056	0.1411	0.5289	0.0361	52.9012
2000	3017.3586	216.8567	4.8555	0.1437	0.5349	0.0364	54.9200
2500	3073.5148	220.8926	4.9482	0.1470	0.5438	0.0370	56.6369
3000	3124.9574	224.5898	4.9870	0.1499	0.5486	0.0371	59.3266
3500	3147.3108	226.1963	4.9760	0.1515	0.5467	0.0368	61.9434
4000	3200.2195	229.9988	4.9977	0.1546	0.5491	0.0366	65.7862
4500	3228.6623	232.0430	4.9585	0.1565	0.5453	0.0359	69.8067
5000	3309.1727	237.8292	4.9577	0.1617	0.5444	0.0352	77.5807
5500	3445.4696	247.6247	5.0186	0.1707	0.5472	0.0349	89.4644
6000	3857.5189	277.2384	5.2460	0.1956	0.5657	0.0345	120.4958

Table III: % Improvement of CV Queue Length Optimization over Fixed Phase Signal Timing, Traffic Volume Sensitivity Analysis Results

Volume (vphpi)	Energy (kJ/veh)	CO2 (g/veh)	CO (g/veh)	HC (g/veh)	NOx (g/veh)	PM2.5 (g/veh)	VHT (s/veh)
1000	14.74%	14.74%	12.51%	17.96%	10.66%	10.00%	32.01%
1500	14.03%	14.03%	9.53%	16.44%	9.03%	5.48%	32.62%
2000	12.04%	12.04%	6.68%	13.74%	6.93%	2.10%	29.78%
2500	10.57%	10.57%	4.23%	11.72%	5.13%	-0.96%	28.27%
3000	9.37%	9.37%	2.17%	10.04%	3.82%	-3.63%	26.58%
3500	8.60%	8.60%	1.06%	8.71%	3.41%	-5.13%	24.25%
4000	8.14%	8.14%	0.50%	8.06%	3.00%	-5.74%	22.85%
4500	7.28%	7.28%	0.11%	6.72%	3.05%	-5.78%	19.06%
5000	5.64%	5.64%	-0.57%	4.37%	2.90%	-5.84%	12.89%
5500	4.23%	4.23%	-1.54%	2.30%	2.50%	-6.59%	7.82%
6000	-0.45%	-0.45%	-3.63%	-3.24%	0.82%	-6.80%	-1.45%

3.4.2 Connected Vehicle Queue Length Signal Optimization versus Webster Signal Timing

The cycle length for the Webster signal timing intersection, as determined by the Webster equation, was applied individually to each traffic volume in order to provide a strong baseline. The CV queue length optimizer is given no information regarding the incoming volume of traffic. However, the Webster signal timing intersection is given information not only on the total volume of incoming traffic, but also which lanes the overall origins and destinations of the incoming vehicles. Accordingly, the signal splits for the Webster signal timing intersection are determined using the OD matrix. In contrast, the signal splits for the CV queue length signal optimization are determined in real-time without any use of *a priori* information.

The results for the queue length CV signal optimizer relative to volume-specific Webster signal timing are shown in Figs. 20-24 and Tables IV-VI. The range of average travel time savings for the CV queue length signal optimization over Webster signal timing falls between -5% and 13%. Previously, the range of average travel time savings for the CV queue length signal optimization over fixed phase signal timing was shown to be between -1% and 32%. The average travel time savings are lower relative to Webster signal timing due to the relative strength of the baseline. In this case, Webster signal timing is a stronger baseline than fixed phase signal timing due to the cycle length being set independently for each traffic volume for the Webster signal timing. As was the case with the comparison with fixed phase signal timing, the average travel time benefits are highest at the lowest traffic volumes. The average travel time savings are negative for traffic volumes greater than or equal to 5000 vehicles per hour. The average energy savings ranged from 0% to about 10%, with the higher range of benefits occurring at the lower traffic volumes. The average emissions savings ranged from -2% to 13%, with the higher range of benefits also occurring at low traffic volumes. In contrast to the comparison with the fixed phase signal timing, the emissions savings are predominantly positive across the tested traffic volumes. The reason for the additional positive savings is due to the difference in cycle lengths between the baselines. The Webster signal timing used cycle lengths that were much shorter than the cycle length of 120 seconds used for the fixed phase signal timing baseline. One of the potential disadvantages of using a shorter cycle length is that the number of vehicle stops increases. An increase in the number of vehicle stops may be shown to be correlated to an increase in vehicle emissions.

Fig. 20: Average Travel Time Comparison of CV Queue Length Signal Optimization and Webster Signal Timing for an Isolated Intersection

Fig. 21: Average Travel Time Percent Savings of CV Queue Length Signal Optimization over Webster Signal Timing on an Isolated Intersection

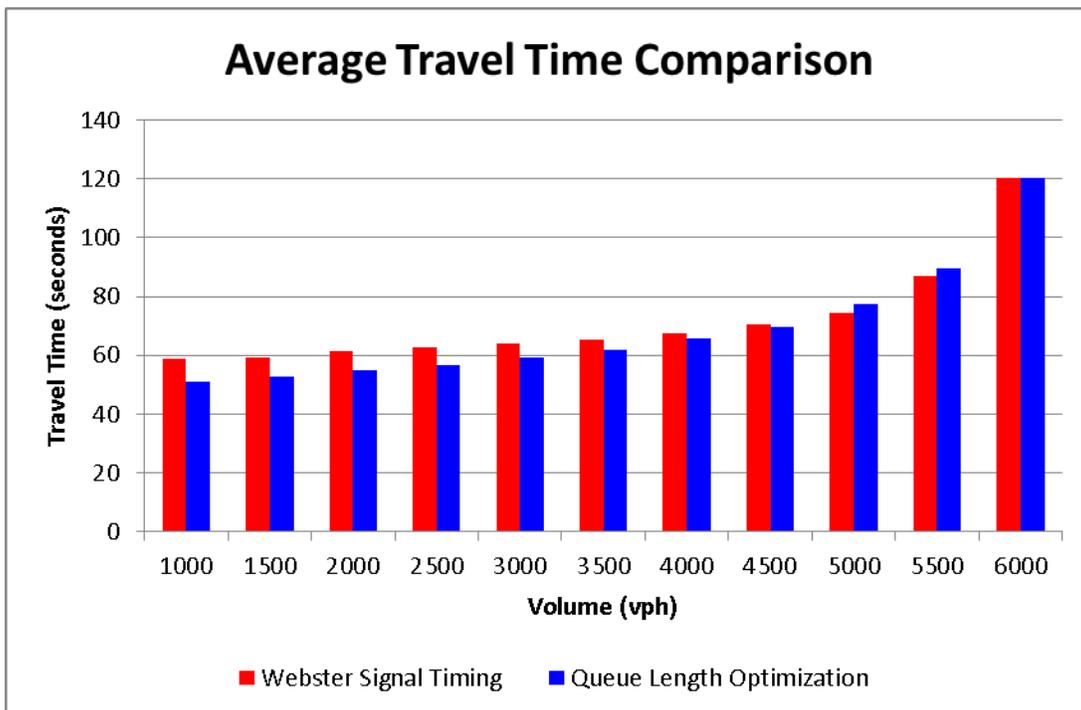Fig. 22: Average Energy Comparison of CV Queue Length Signal Optimization and Webster Signal Timing for an Isolated Intersection
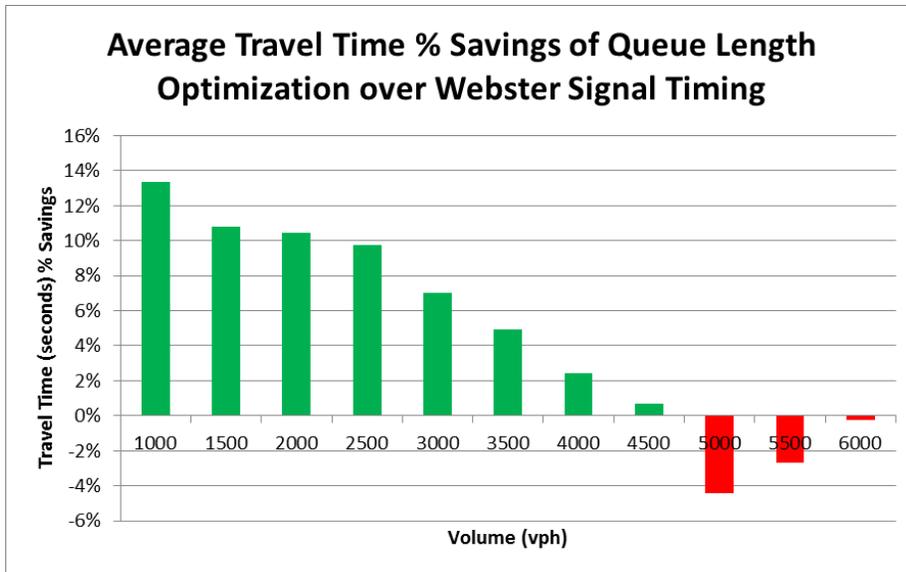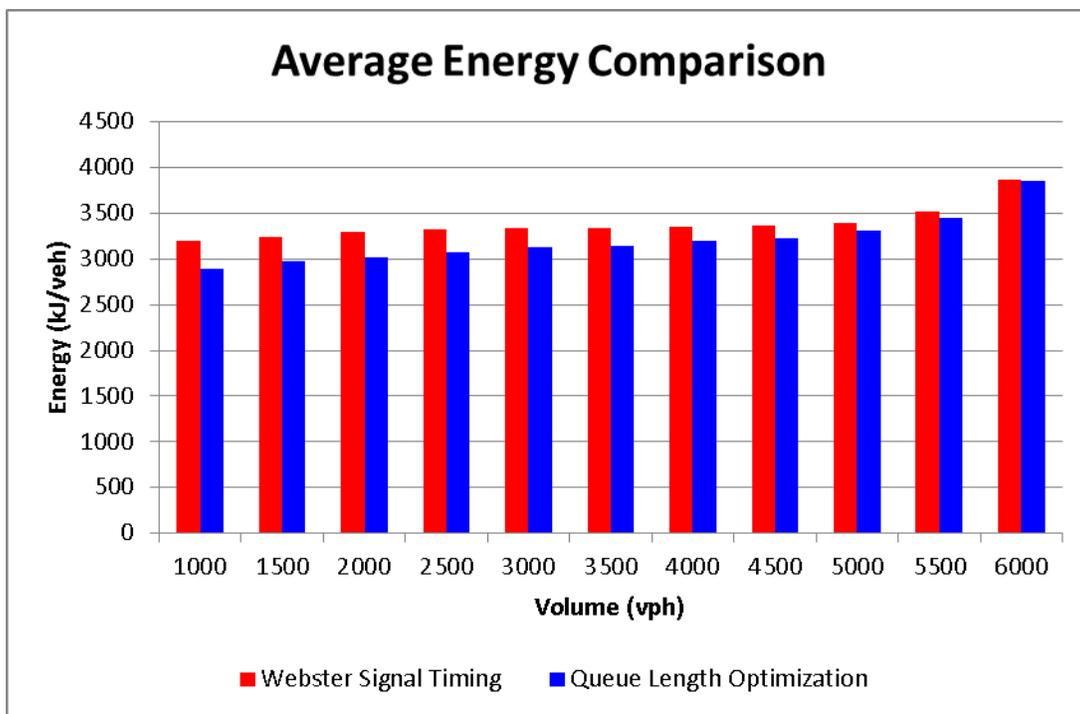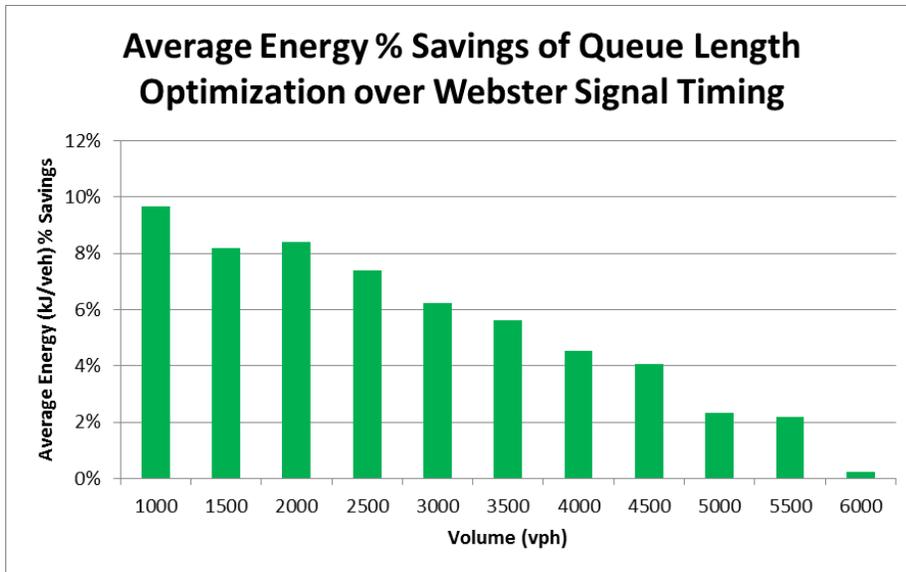
Fig. 23: Average Energy Percent Savings of CV Queue Length Signal Optimization over Webster Signal Timing on an Isolated Intersection
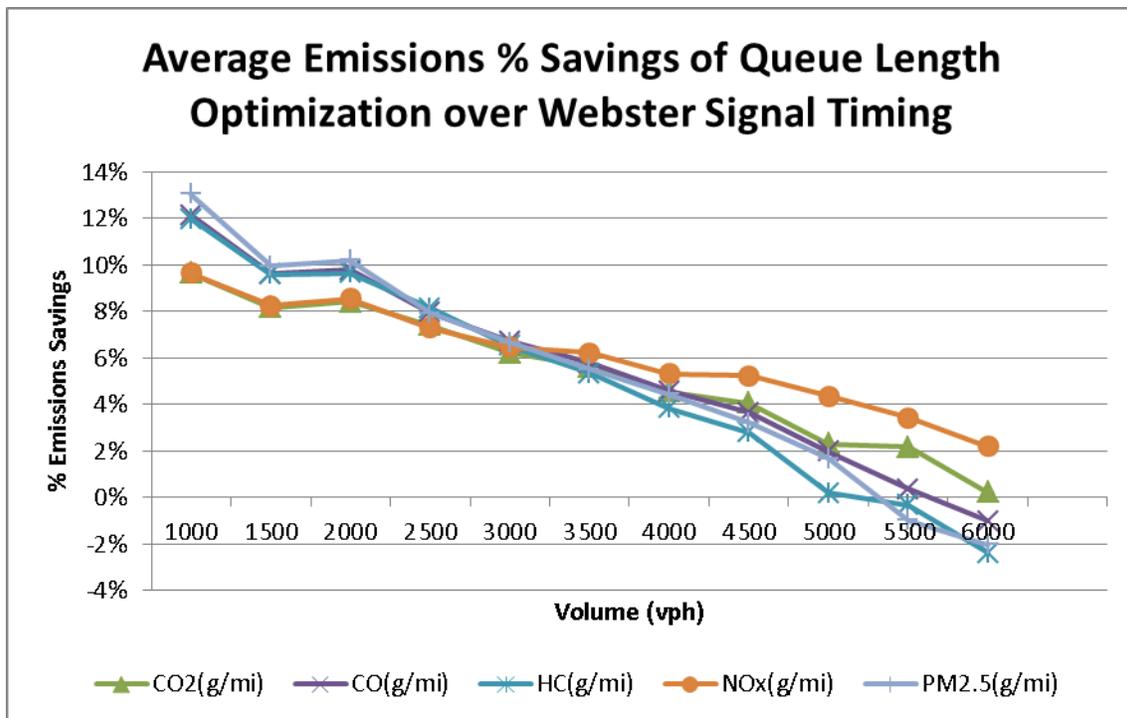

Fig. 24: Average Emissions Percent Savings of CV Queue Length Signal Optimization over Webster Signal Timing on an Isolated Intersection

Table IV: Webster Signal Timing, Traffic Volume Sensitivity Analysis Results

Volume (vphpi)	Energy (kJ/veh)	CO2 (g/veh)	CO (g/veh)	HC (g/veh)	NOx (g/veh)	PM2.5 (g/veh)	VHT (s/veh)
1000	3197.8442	229.8281	5.3001	0.1549	0.5694	0.0402	58.7392
1500	3234.6362	232.4724	5.3175	0.1561	0.5764	0.0401	59.2864
2000	3294.6454	236.7852	5.3830	0.1591	0.5849	0.0405	61.3116
2500	3319.0298	238.5377	5.3760	0.1601	0.5866	0.0402	62.7683
3000	3332.7369	239.5228	5.3459	0.1604	0.5866	0.0397	63.7971
3500	3335.0394	239.6883	5.2817	0.1601	0.5831	0.0389	65.1727
4000	3352.5423	240.9462	5.2377	0.1608	0.5800	0.0383	67.4273
4500	3365.7337	241.8943	5.1466	0.1611	0.5755	0.0371	70.2974
5000	3387.5355	243.4611	5.0575	0.1620	0.5693	0.0358	74.2839
5500	3522.0480	253.1284	5.0368	0.1701	0.5668	0.0346	87.1314
6000	3866.3465	277.8729	5.1936	0.1910	0.5784	0.0338	120.2226

Table V: CV Queue Length Signal Optimization, Traffic Volume Sensitivity Analysis Results

Volume (vphpi)	Energy (kJ/veh)	CO2 (g/veh)	CO (g/veh)	HC (g/veh)	NOx (g/veh)	PM2.5 (g/veh)	VHT (s/veh)
1000	2888.9053	207.6249	4.6571	0.1364	0.5145	0.0350	50.8897
1500	2970.3667	213.4795	4.8056	0.1411	0.5289	0.0361	52.9012
2000	3017.3586	216.8567	4.8555	0.1437	0.5349	0.0364	54.9200
2500	3073.5148	220.8926	4.9482	0.1470	0.5438	0.0370	56.6369
3000	3124.9574	224.5898	4.9870	0.1499	0.5486	0.0371	59.3266
3500	3147.3108	226.1963	4.9760	0.1515	0.5467	0.0368	61.9434
4000	3200.2195	229.9988	4.9977	0.1546	0.5491	0.0366	65.7862
4500	3228.6623	232.0430	4.9585	0.1565	0.5453	0.0359	69.8067
5000	3309.1727	237.8292	4.9577	0.1617	0.5444	0.0352	77.5807
5500	3445.4696	247.6247	5.0186	0.1707	0.5472	0.0349	89.4644
6000	3857.5189	277.2384	5.2460	0.1956	0.5657	0.0345	120.4958

Table VI: % Improvement of CV Queue Length Optimization over Webster Signal Timing, Traffic Volume Sensitivity Analysis Results

Volume (vphpi)	Energy (kJ/veh)	CO2 (g/veh)	CO (g/veh)	HC (g/veh)	NOx (g/veh)	PM2.5 (g/veh)	VHT (s/veh)
1000	9.66%	9.66%	12.13%	11.98%	9.65%	13.04%	13.36%
1500	8.17%	8.17%	9.63%	9.60%	8.24%	9.95%	10.77%
2000	8.42%	8.42%	9.80%	9.64%	8.55%	10.20%	10.42%
2500	7.40%	7.40%	7.96%	8.15%	7.29%	7.93%	9.77%
3000	6.23%	6.23%	6.71%	6.52%	6.47%	6.66%	7.01%
3500	5.63%	5.63%	5.79%	5.36%	6.24%	5.51%	4.96%
4000	4.54%	4.54%	4.58%	3.85%	5.33%	4.43%	2.43%
4500	4.07%	4.07%	3.65%	2.81%	5.24%	3.21%	0.70%
5000	2.31%	2.31%	1.97%	0.20%	4.37%	1.68%	-4.44%
5500	2.17%	2.17%	0.36%	-0.32%	3.44%	-0.97%	-2.68%
6000	0.23%	0.23%	-1.01%	-2.38%	2.19%	-2.01%	-0.23%

3.5 Demand Profile Sensitivity Analysis

An additional sensitivity analysis was performed on the demand profile of traffic arriving at the intersections. A demand profile is a sequence that can modify an OD matrix to provide additional traffic during specified time intervals. For example, a sequence such as {25, 25, 25, 25} specifies that 25% of the traffic for a given OD pair should be released by the simulator during the first quarter of the simulation time period. A demand profile of {100} leaves the OD matrix unmodified. For the demand profile sensitivity test, the volume to capacity ratio was set to 0.5 for each signal control strategy, and demand profile sequences with standard deviations of 1, 3, and 5 were tested relative to a demand profile of {100}. The specific demand profile sequences are shown in Table VII. The individual numbers in the demand profile sequences with non-zero standard deviation specify the percentage of the overall hourly volume for OD pairs for specific 5-minute intervals. The first number in the sequence specifies the first 5-minute interval during the hour-long simulation run. Although the overall hourly volume is set to 0.5 times the V/C ratio, the 5-minute interval volumes each have their own V/C ratio. The individual sequence numbers were constrained to ensure that the 5-minute interval V/C ratios did not exceed 1. The signal splits for the fixed phase signal timing were set with the assumption that the ratios of traffic utilizing each signal phase were known perfectly *a priori*. Likewise, both the cycle length and the signal splits for the HCM and Webster signal timing were set with perfect *a priori* knowledge. The signal timing for the CV queue length signal optimization was not based on the availability of the OD matrix, and was instead calculated in real-time during the simulation.

The relative percent sensitivity results are shown in Fig. 25 and Table VIII below, where the results are measured relative to a demand profile with a standard deviation of 0. The fixed phase signal timing strategy was the least sensitive to increases in the variation of the demand profile. The HCM signal timing strategy exhibited the highest relative sensitivity at the highest standard deviation tested. An additional method of analyzing sensitivity is to observe the absolute values

of travel times for different demand profiles. Accordingly, absolute travel time sensitivity results are shown in Fig. 26 and Table IX below. When viewed through the perspective of absolute travel times, it becomes evident that the CV queue length signal optimization strategy has the lowest travel time across all of the demand profiles tested. Although the fixed phase signal timing was the least sensitive in terms of relative percent sensitivity, fixed phase signal timing was generally the worst in terms of absolute travel time.

Table VII: Demand Profile Sequences used for Demand Profile Sensitivity Test

Standard Deviation of Demand Profile	Demand Profile Sequence
0	{100}
1	{8, 8, 7, 8, 9, 8, 10, 7, 9, 8, 10, 8}
3	{3, 9, 7, 12, 6, 14, 8, 7, 7, 11, 9, 7}
5	{3, 12, 4, 11, 13, 17, 5, 7, 3, 3, 14, 8}

Fig. 25: Percent Travel Time Sensitivity to Varied Demand Profile

Table VII: Percent Travel Time Sensitivity to Varied Demand Profile

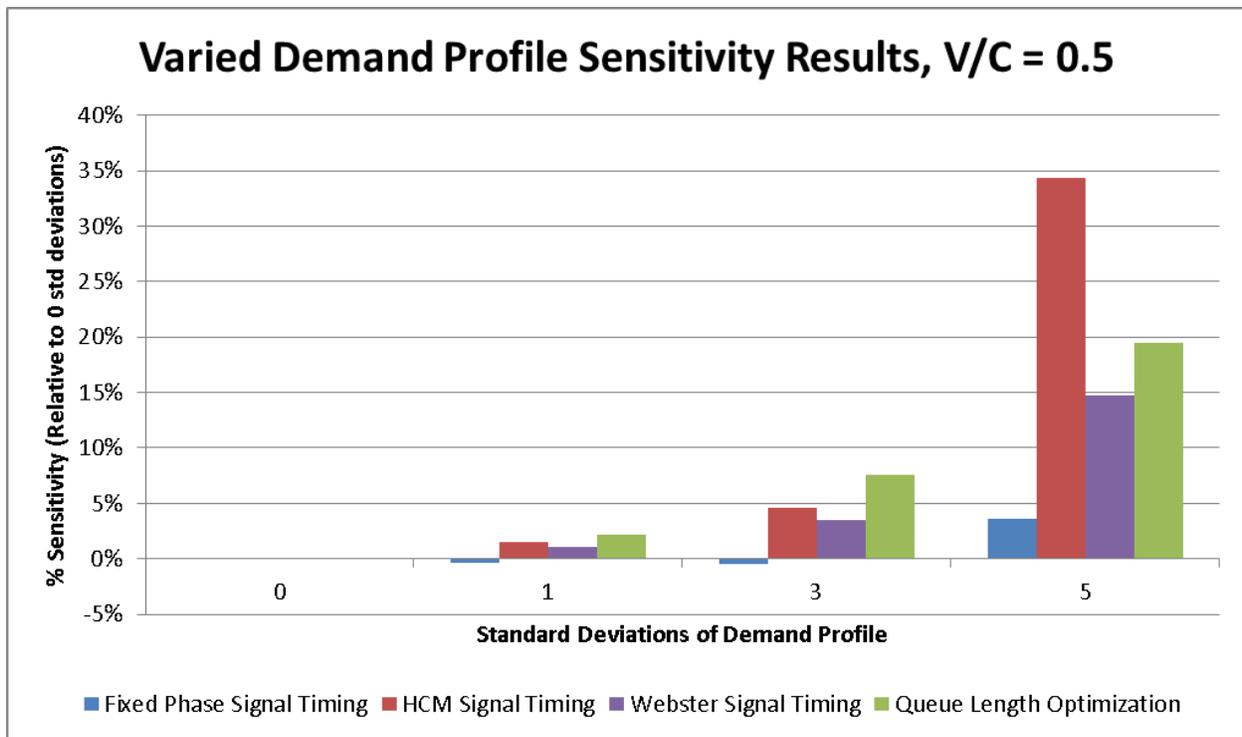|		Signal Timing Method			
		Fixed Phase	HCM	Webster	CV Queue Length Optimization
Standard Deviations of Demand Profile	0	---	---	---	---
	1	0%	1%	1%	2%
	3	0%	5%	3%	8%
	5	4%	34%	15%	19%
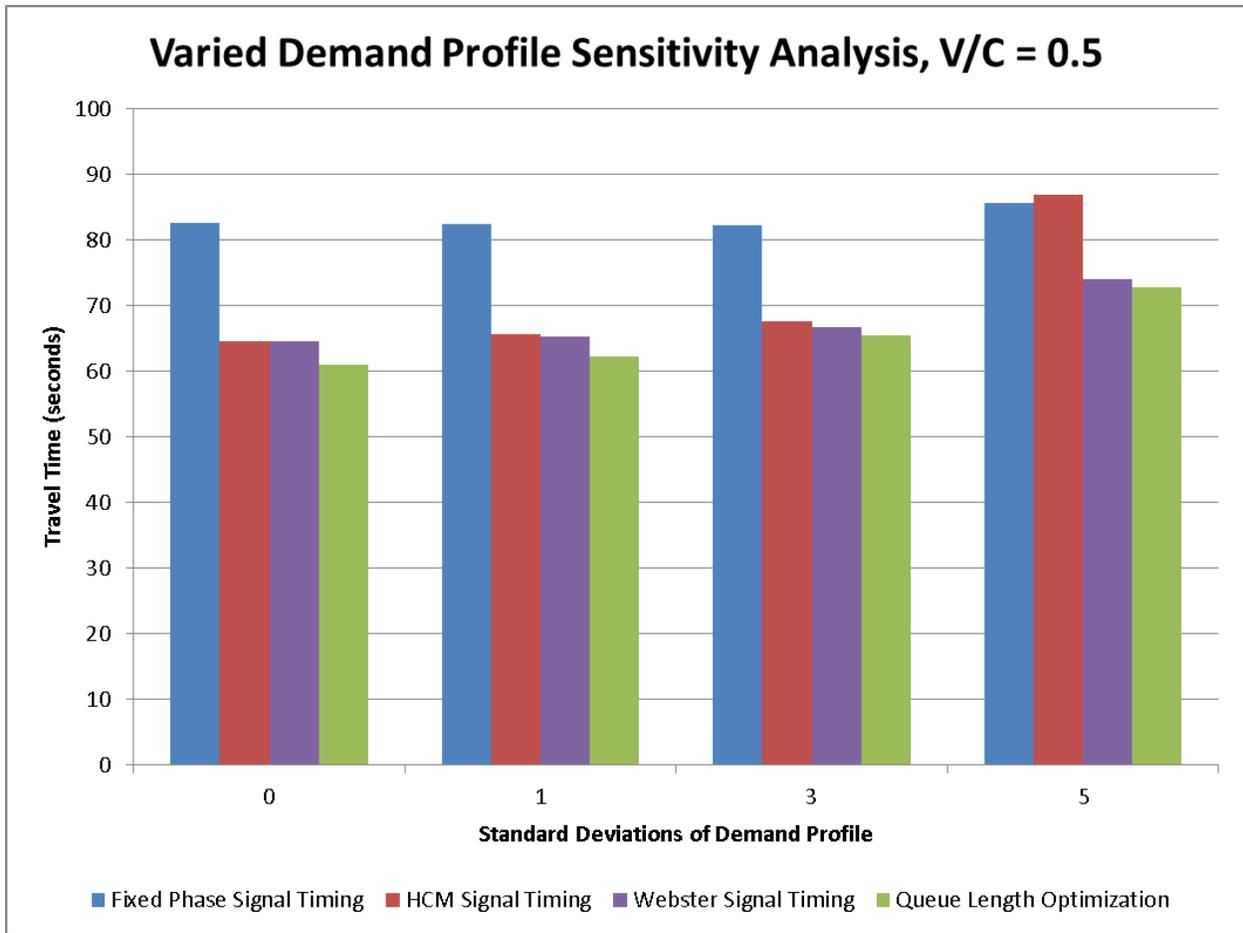
Fig. 26: Travel Time Sensitivity to Varied Demand Profile

Table IX: Travel Time Sensitivity to Varied Demand Profile

		Signal Timing Method			
		Fixed Phase	HCM	Webster	CV Queue Length Optimization
Standard Deviations of Demand Profile	0	82.6888	64.6436	64.5542	60.9619
	1	82.3683	65.5899	65.2621	62.2486
	3	82.2838	67.6122	66.8010	65.5581
	5	85.6539	86.8335	74.0670	72.8055

4. Corridor-Level Connected Vehicle Signal Optimization

4.1 Application Description

The CV queue length signal optimizer described in the previous chapter in the context of an isolated intersection may readily be extended to multiple intersections. A sequence of intersections may be referred to as a signalized corridor. Traditionally, signalized corridors are operated using a coordinated fixed phase signal timing where the intersections share the same signal timing plan with time offsets based on the physical distance between subsequent intersections. The coordinated fixed phase signal timing plan is designed to permit vehicles traveling along the corridor to be able to travel through multiple intersections without stopping. In the case of adaptive signal control, a given intersections signal plan is unfixed. Consequently, one method for extending the CV queue length signal optimizer from an isolated intersection to a corridor of intersections is to apply the same optimizer to each intersection. Each intersection is set to operate independently of adjacent intersections, constituting what may be referred to as decentralized corridor management. The following sections will describe the implementation, testing, and results of simulating a decentralized signalized corridor in a CV environment.

4.2 Simulation Setup

As with the case of the isolated intersection, PARAMICS 6.9.3 [19] was also used to simulate a corridor of three signalized intersections. The PARAMICS API provided access to mobility results, and EPA's MOVES [20] provided emissions results. The OD matrix for a corridor of three intersections was set such that each intersection would retain the same level of traffic as the single isolated intersection described in section 3.3. Instead of using fixed turning ratios and a fixed ratio of major to minor street traffic, a custom OD matrix generator was developed to allow these values to vary every 5 minutes to better reflect the variations in real-world traffic. In addition, a demand profile with a standard deviation of 1 was used to further emulate real-world traffic. Accordingly, the ratio of major street to minor street traffic was set to 1.5 with a standard deviation of 0.2. The percentage of left-turn movement traffic was set to 20% with a standard deviation of 0.05. Likewise, the percentage of through movement traffic was set to 70% with a standard deviation of 0.05. All remaining traffic, roughly 10%, was set to be right-turn movement traffic. In addition, the ratio of traffic originating from the north to traffic originating from the south was set to 1.05 with a standard deviation of 0.1. Likewise, the ratio of traffic originating from the west to traffic originating from the east was set to 1.05 with a standard deviation of 0.1. Using the input values mentioned above a set of 12 OD matrices were generated, one for every 5-minute interval. Each simulation run was conducted for 1 hour with additional time for vehicles to clear the network.

4.3 PARAMICS Network Description

The PARAMICS network for a corridor of 3 intersections is shown in Fig. 27 below. Each intersection is identical to the isolated intersection described in section 3.3. The distance between the stop bars of successive intersections was set to 2415 feet. The speed limit throughout the network was set at 45 mph. Based on the distance between intersections and the speed limit, the progression time, (the time a vehicle takes to get from one intersection to the next), was calculated to be 37 seconds. For the baseline coordinated fixed phase signal timing

network, the cycle length which permits the largest "green window" for coordinating East-West and West-East traffic was 74 seconds. The phrase "green window" refers to the time duration allotted during a cycle to coordinated movements between multiple intersections. Based on a complete knowledge of the OD matrix, the effective "green window," (the coordinated green phase duration plus 2 seconds of yellow), was set to 18 seconds out of the 74-second cycle. The left and right intersections depicted in Fig. 27 operate with a time offset of 0 seconds. The center intersection shown in the figure operates with a time offset of 37 seconds. A time-space diagram, shown in Fig. 28, summarizes the baseline coordinated fixed phase signal timing plan for the 3-intersection corridor. The decentralized CV queue length signal optimization network operated without the use of a predetermined signal timing plan. Each intersection was permitted to determine its own signal timing based on the vehicles within range of the given intersection. The communication radius for each intersection, (~600 feet), was set to fully overlap the beginning of the left-turn bays for the purpose of the intersection being able to distinguish between left-turn movement traffic and through movement traffic. If the communication radius is set shorter, then the IMA is less informed in its optimization of signal timing. If the communication radius is expanded beyond the length of the left-turn bay, then vehicles are required to communicate their turning intentions to the IMA. Transmitting turning intentions may be viewed as a violation of driver privacy.

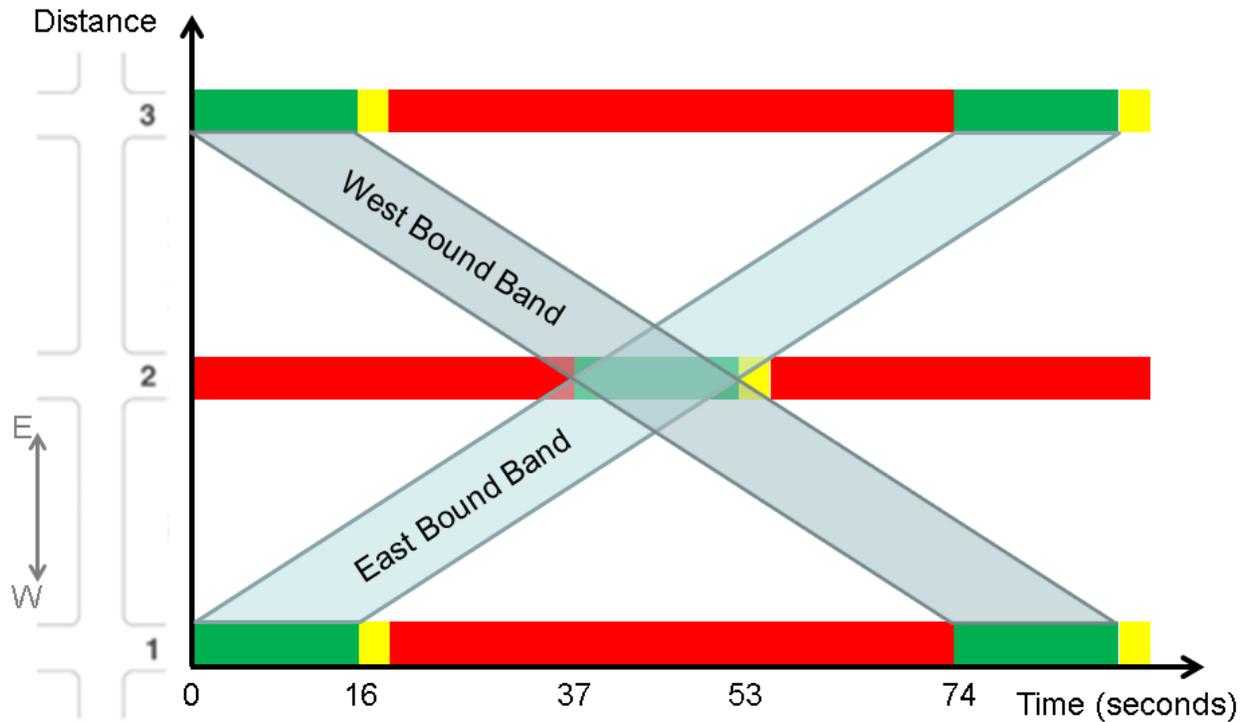Fig. 27: 3-Intersection Corridor PARAMICS Network

Fig. 28: Time-Space Diagram showing Coordinated Fixed Phase Signal Timing Plan for PARAMICS Network (see previous Fig.)

4.4 Volume Sensitivity Analysis

For the volume sensitivity analysis, a series of traffic volumes ranging from 1000 vehicle per hour per intersection (vphpi) to 6000 vphpi in 500 vphpi increments was tested. The average corridor level results are shown in Figs. 29-33 and Tables X-XII. The decentralized CV queue length signal optimizer outperforms the coordinated fixed phase signal timing for traffic volumes less than or equal to 4000 vphpi. The maximum average travel time savings of 19% was achieved at the lowest volume tested (1000 vphpi). Similarly, the maximum average energy savings of nearly 8% was achieved at the same volume. As the traffic volume was increased, average travel time, energy, and emissions savings decreased. At traffic volumes greater than 4000 vphpi, the average travel time and energy savings were negative, reaching minimums of -22% and -8%, respectively. Emissions savings were for the most part negative, varying predominantly between -10% and +10%, with the positive savings occurring at the low traffic volumes.

Additional insight can be gained by dividing the results into the categories of coordinated-phase vehicles and uncoordinated-phase vehicles. Coordinated-phase vehicles are defined as vehicles which travel the full length of the corridor. Examining coordinated-phase vehicle statistics helps determine if, and to what extent, coordinated-phase vehicles are negatively impacted by passing through independently adaptive intersections instead of progressing through a coordinated fixed phase signal timing corridor. The coordinated-phase vehicle results are shown in Figs. 34-38 and Tables XIII-XV, and are followed by uncoordinated-phase vehicle results which are shown in Figs.

39-43 and Tables XVI-XVIII. A comparison of the average results, the coordinated-phase vehicle results, and the uncoordinated-phase vehicle results is shown in Figs. 44-45.

As hypothesized, the use of decentralized adaptive signal control negatively impacted the average travel time, energy consumption, and emissions of vehicles traveling the full length of the signalized corridor. At the lowest traffic volume tested, (1000 vphpi), there is a small, (less than 2%), benefit in terms of travel time, energy consumption, and emissions. The reason for the small benefit is that vehicles operating under coordinated fixed phase signal timing must wait until the coordinated phase begins. Once the coordinated phase begins, vehicles are able to progress through the remaining two intersections with relatively little delay. In contrast, vehicles operating under decentralized adaptive signal timing experience a certain amount of delay at each of the three intersections. At the traffic volume of 1000 vphpi, the average delay experienced by vehicles passing through the three decentralized adaptive signal timing intersections was slightly less than the average delay experience by vehicles waiting for the coordinated phase to begin in the coordinated fixed phase signal timing corridor. For traffic volumes greater than 1000 vphpi, the average delay per intersection summed over the three intersections for the decentralized adaptive signal timing corridor outweighs the average delay experienced by vehicles waiting for the start of the coordinated phase in the coordinated fixed phase signal timing baseline corridor. The penalty experienced by traffic traveling through the length of the corridor increases with volume and reaches a maximum of -59% in terms of travel time and -19% in terms of energy.

In contrast to the coordinated-phase vehicles, the uncoordinated-phase vehicles generally experience benefits under decentralized adaptive signal control relative to coordinated fixed phase signal timing. The maximum uncoordinated-phase vehicle benefits of 23% for travel time and 9% for energy occur at a traffic volume of 1000 vphpi. The benefits decrease with volume, remaining positive up to 4500 vphpi. The benefits are negative for traffic volumes greater than 4500 vphpi. The emissions savings for uncoordinated-phase vehicles are in the 0% to 10% range for traffic volumes less than or equal to 2500 vphpi. Examining the average, coordinated-phase, and uncoordinated-phase vehicle statistics reveals that the overall average is lowered by the relatively poor performance of coordinated-phase vehicles in the decentralized adaptive signal control corridor. However, the overall benefits are still positive for traffic volumes up to 4000 vphpi due to the positive benefits experienced by uncoordinated-phase vehicles.
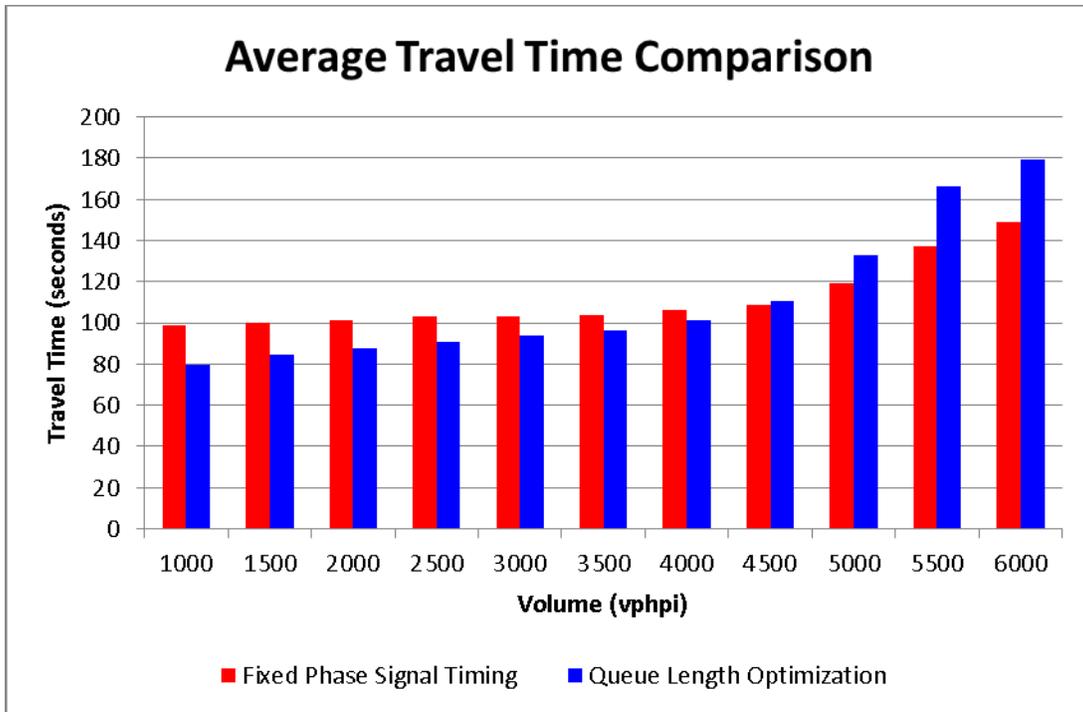
Fig. 29: Average Travel Time Comparison of Decentralized CV Queue Length Signal Optimization and Coordinated Fixed Phase Signal Timing for a 3-intersection Corridor
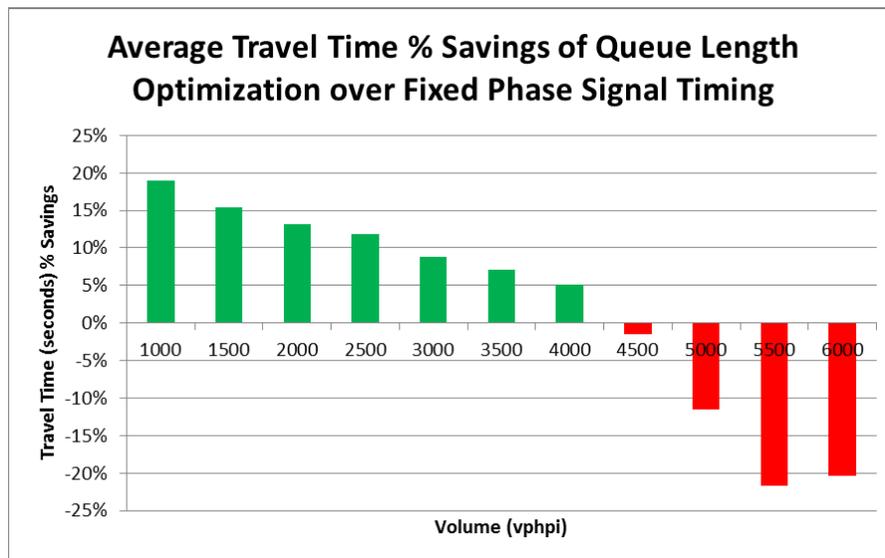

Fig. 30: Average Travel Time Percent Savings of Decentralized CV Queue Length Signal Optimization over Coordinated Fixed Phase Signal Timing on a 3-intersection Corridor
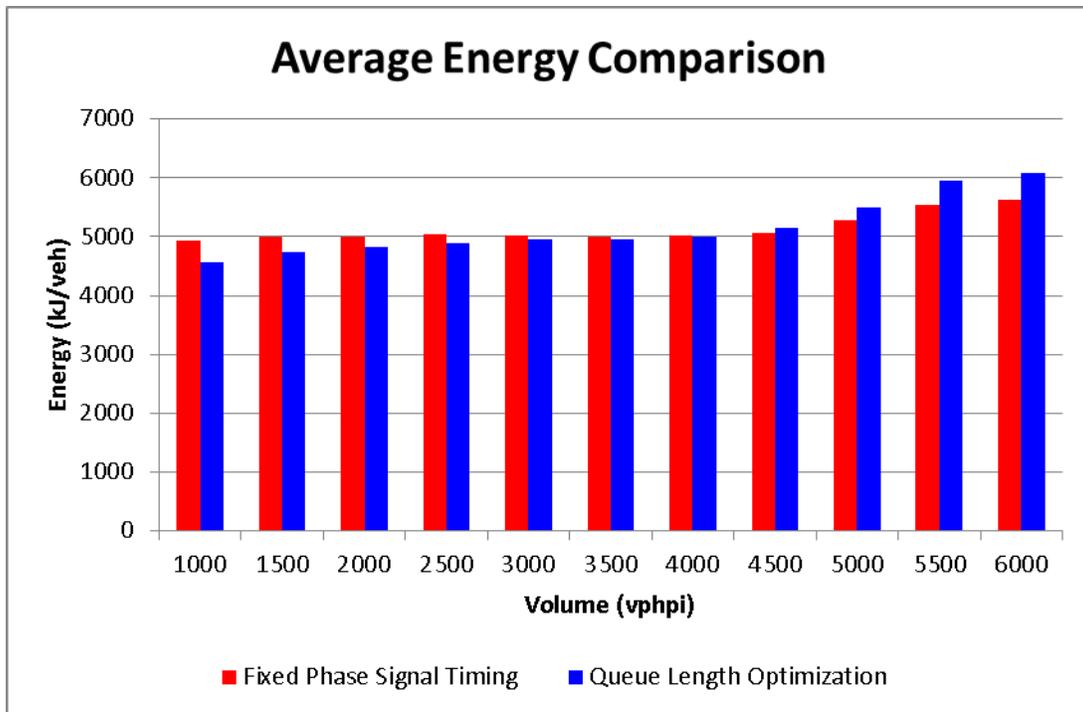
Fig. 31: Average Energy Comparison of Decentralized CV Queue Length Signal Optimization and Coordinated Fixed Phase Signal Timing for a 3-intersection Corridor
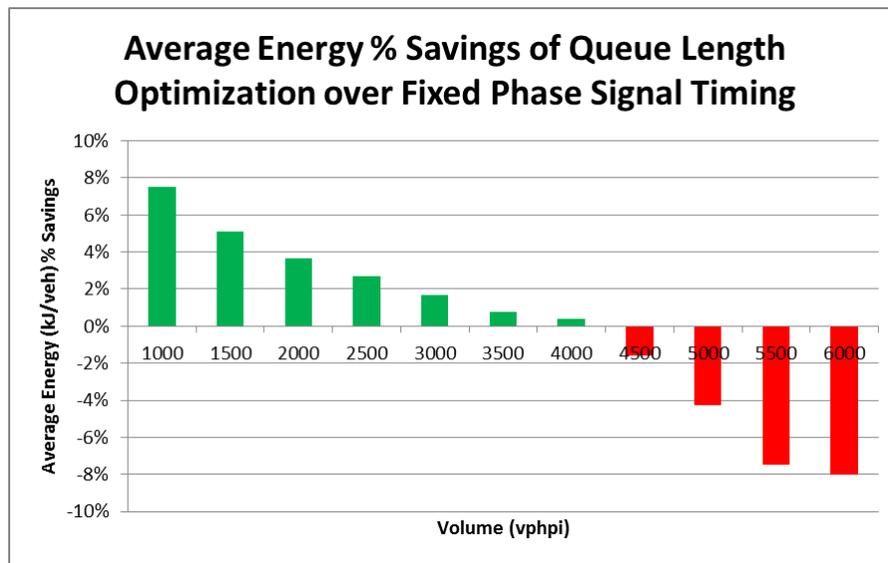

Fig. 32: Average Energy Percent Savings of Decentralized CV Queue Length Signal Optimization over Coordinated Fixed Phase Signal Timing on a 3-intersection Corridor
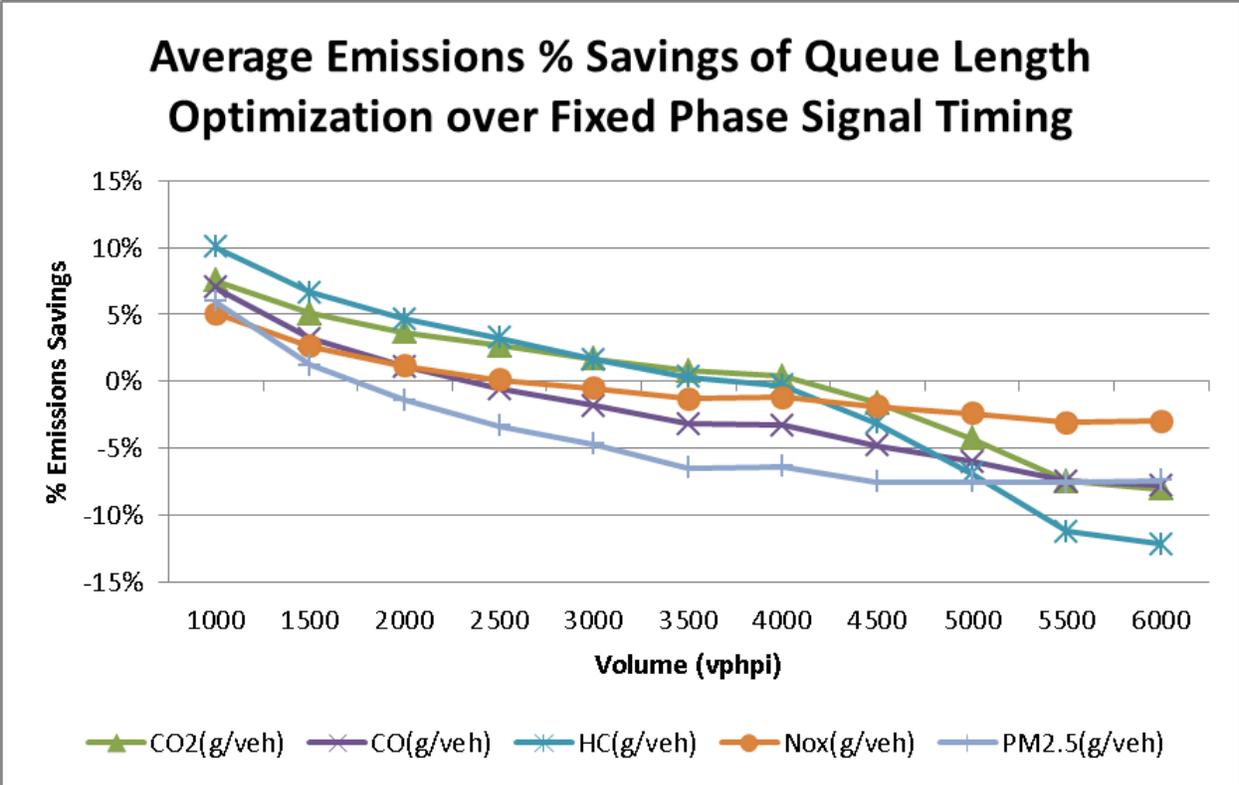
Fig. 33: Average Emissions Percent Savings of Decentralized CV Queue Length Signal Optimization over Coordinated Fixed Phase Signal Timing on a 3-intersection Corridor

Table X: Coordinated Fixed Phase Signal Timing, Traffic Volume Sensitivity Analysis Results

Volume (vphpi)	Energy (kJ/veh)	CO2 (g/veh)	CO (g/veh)	HC (g/veh)	NOx (g/veh)	PM2.5 (g/veh)	VHT (s/veh)
1000	4925.0679	353.9632	7.3467	0.2324	0.8340	0.0525	98.6335
1500	5000.7984	359.4060	7.4100	0.2353	0.8462	0.0526	100.0019
2000	5003.7649	359.6192	7.3507	0.2351	0.8434	0.0519	101.0038
2500	5031.3857	361.6042	7.3500	0.2367	0.8442	0.0516	102.9197
3000	5026.5534	361.2569	7.3021	0.2360	0.8426	0.0510	102.8570
3500	4993.5554	358.8854	7.2024	0.2345	0.8332	0.0500	103.5022
4000	5015.0644	360.4312	7.2067	0.2365	0.8313	0.0499	106.4753
4500	5064.1490	363.9589	7.2211	0.2387	0.8356	0.0496	108.6725
5000	5275.9349	379.1798	7.4089	0.2503	0.8557	0.0503	119.1899
5500	5538.6240	398.0591	7.5681	0.2656	0.8707	0.0502	136.9902
6000	5623.3941	404.1515	7.5606	0.2707	0.8696	0.0495	149.1811

Table XI: Decentralized CV Queue Length Signal Optimization, Traffic Volume Sensitivity Analysis Results

Volume (vphpi)	Energy (kJ/veh)	CO2 (g/veh)	CO (g/veh)	HC (g/veh)	NOx (g/veh)	PM2.5 (g/veh)	VHT (s/veh)
1000	4555.3127	327.3892	6.8316	0.2090	0.7916	0.0494	79.8905
1500	4746.6884	341.1433	7.1728	0.2197	0.8240	0.0520	84.6244
2000	4820.7921	346.4691	7.2716	0.2241	0.8337	0.0527	87.6669
2500	4896.2985	351.8957	7.3917	0.2290	0.8435	0.0534	90.6824
3000	4943.6683	355.3001	7.4348	0.2322	0.8469	0.0534	93.8211
3500	4955.5583	356.1546	7.4336	0.2338	0.8440	0.0532	96.1943
4000	4996.1249	359.0701	7.4459	0.2372	0.8414	0.0531	101.0808
4500	5145.1674	369.7817	7.5682	0.2462	0.8514	0.0534	110.2949
5000	5501.8461	395.4159	7.8531	0.2677	0.8761	0.0541	132.9384
5500	5951.9169	427.7622	8.1354	0.2955	0.8974	0.0540	166.6054
6000	6074.7658	436.5912	8.1514	0.3037	0.8955	0.0532	179.5833

Table XII: % Improvement of Decentralized CV Queue Length Optimization over Coordinated Fixed Phase Signal Timing, Traffic Volume Sensitivity Analysis Results

| Volume (vphpi)	Energy (kJ/veh)	CO2 (g/veh)	CO (g/veh)	HC (g/veh)	NOx (g/veh)	PM2.5 (g/veh)	VHT (s/veh)
1000	7.51%	7.51%	7.01%	10.04%	5.09%	5.95%	19.00%
1500	5.08%	5.08%	3.20%	6.62%	2.62%	1.21%	15.38%
2000	3.66%	3.66%	1.08%	4.68%	1.14%	-1.43%	13.20%
2500	2.68%	2.68%	-0.57%	3.27%	0.08%	-3.35%	11.89%
3000	1.65%	1.65%	-1.82%	1.63%	-0.51%	-4.68%	8.78%
3500	0.76%	0.76%	-3.21%	0.30%	-1.29%	-6.49%	7.06%
4000	0.38%	0.38%	-3.32%	-0.32%	-1.21%	-6.38%	5.07%
4500	-1.60%	-1.60%	-4.81%	-3.16%	-1.88%	-7.52%	-1.49%
5000	-4.28%	-4.28%	-6.00%	-6.93%	-2.39%	-7.54%	-11.53%
5500	-7.46%	-7.46%	-7.49%	-11.24%	-3.07%	-7.58%	-21.62%
6000	-8.03%	-8.03%	-7.81%	-12.21%	-2.98%	-7.45%	-20.38%
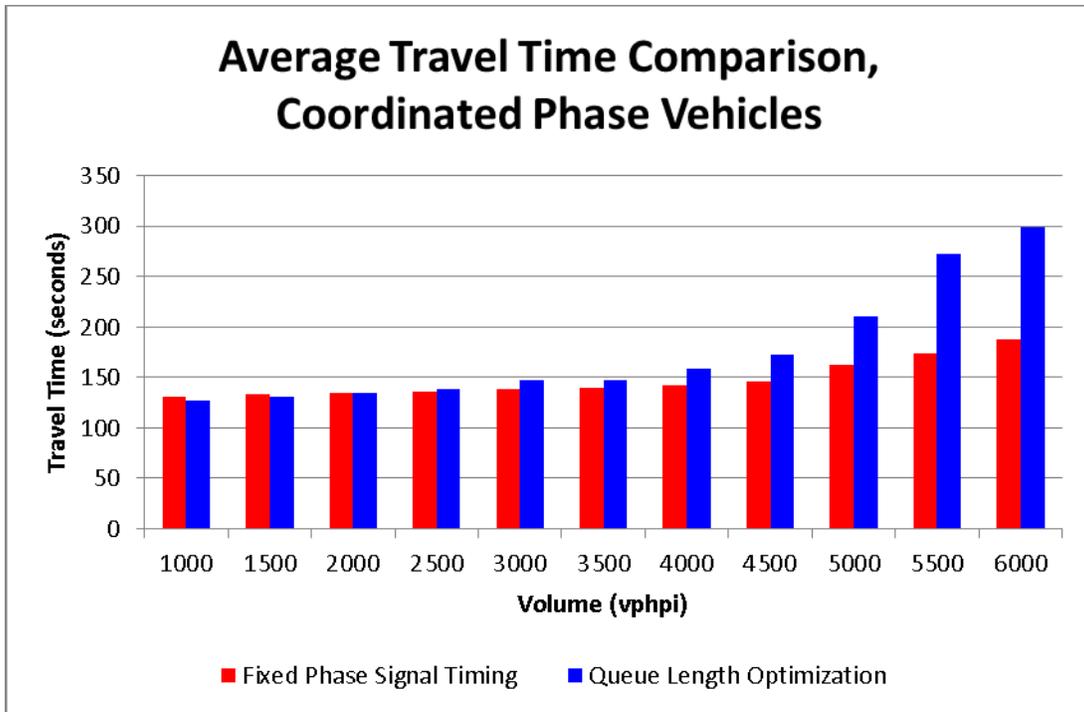
Fig. 34: Coordinated Phase Vehicle Travel Time Comparison of Decentralized CV Queue Length Signal Optimization and Coordinated Fixed Phase Signal Timing for a 3-intersection Corridor
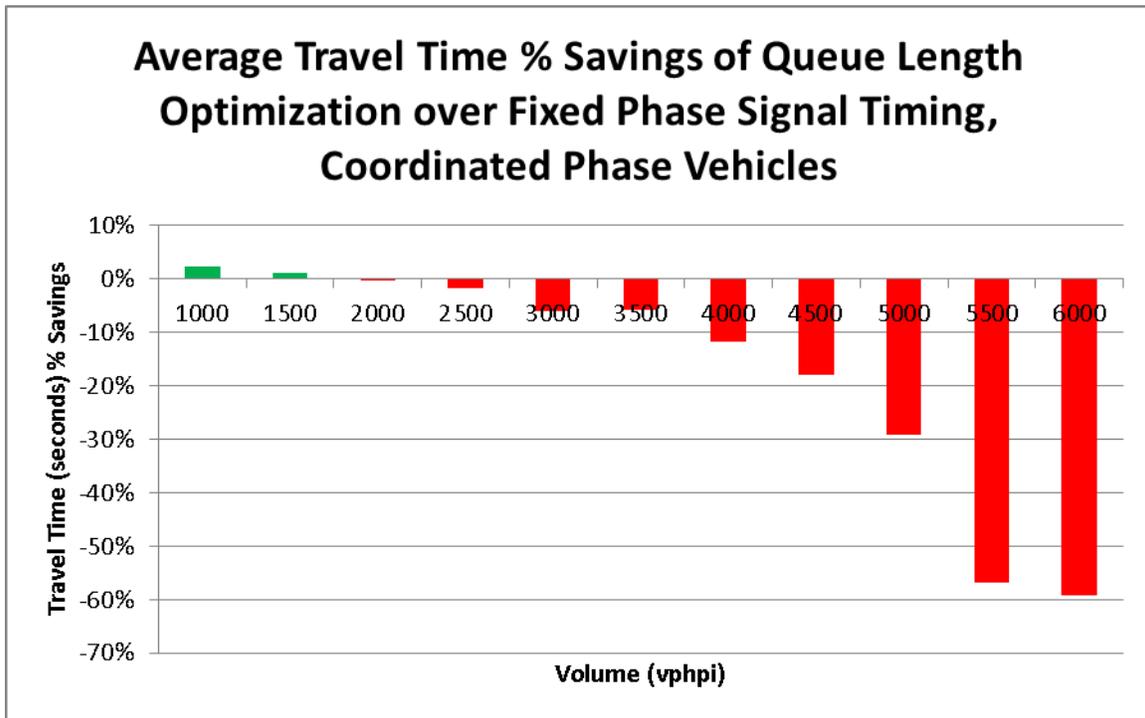

Fig. 35: Coordinated Phase Vehicle Travel Time Percent Savings of Decentralized CV Queue Length Signal Optimization over Coordinated Fixed Phase Signal Timing on a 3-intersection Corridor
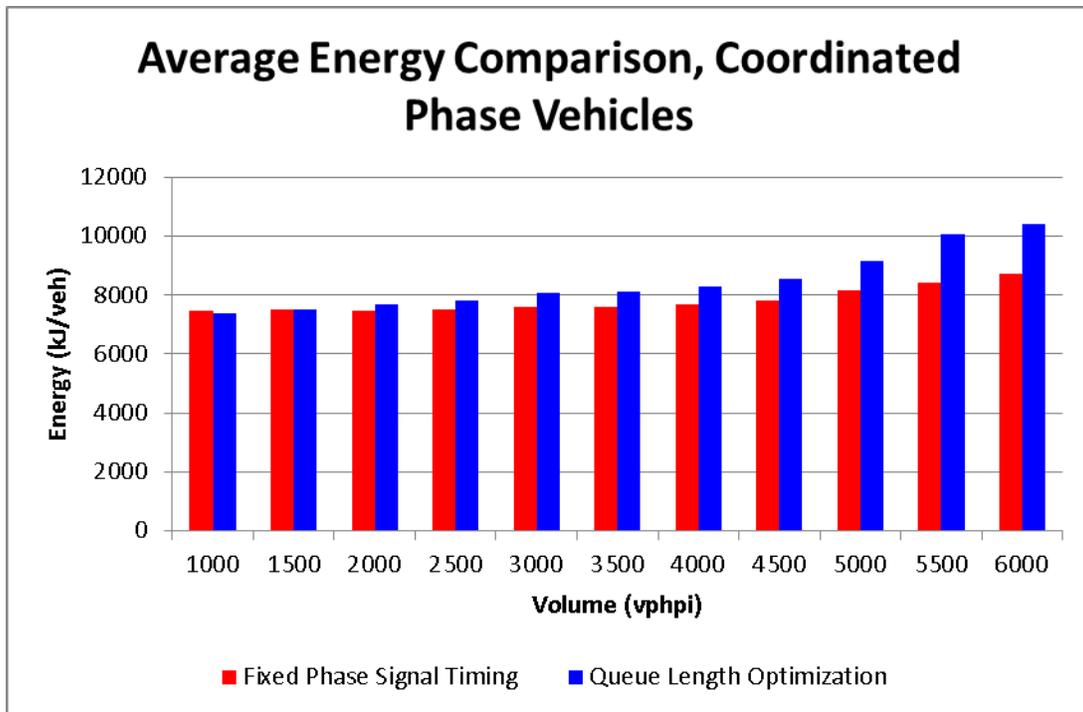
Fig. 36: Coordinated Phase Vehicle Energy Comparison of Decentralized CV Queue Length Signal Optimization and Coordinated Fixed Phase Signal Timing for a 3-intersection Corridor
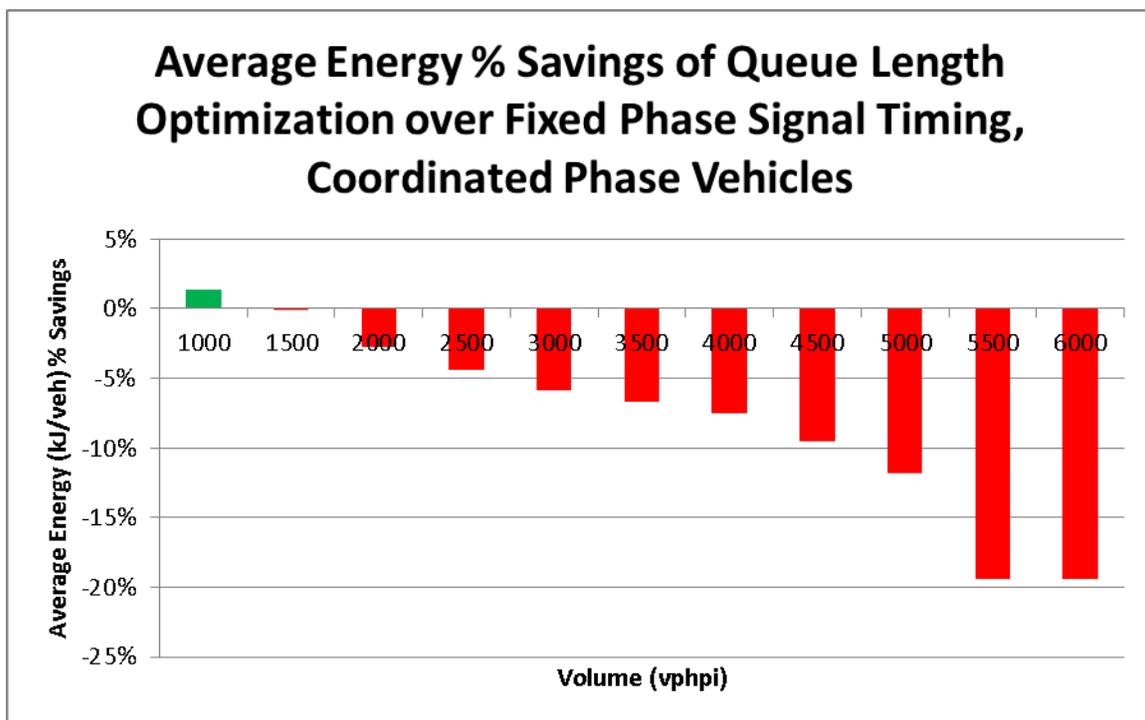

Fig. 37: Coordinated Phase Vehicle Energy Percent Savings of Decentralized CV Queue Length Signal Optimization over Coordinated Fixed Phase Signal Timing on a 3-intersection Corridor
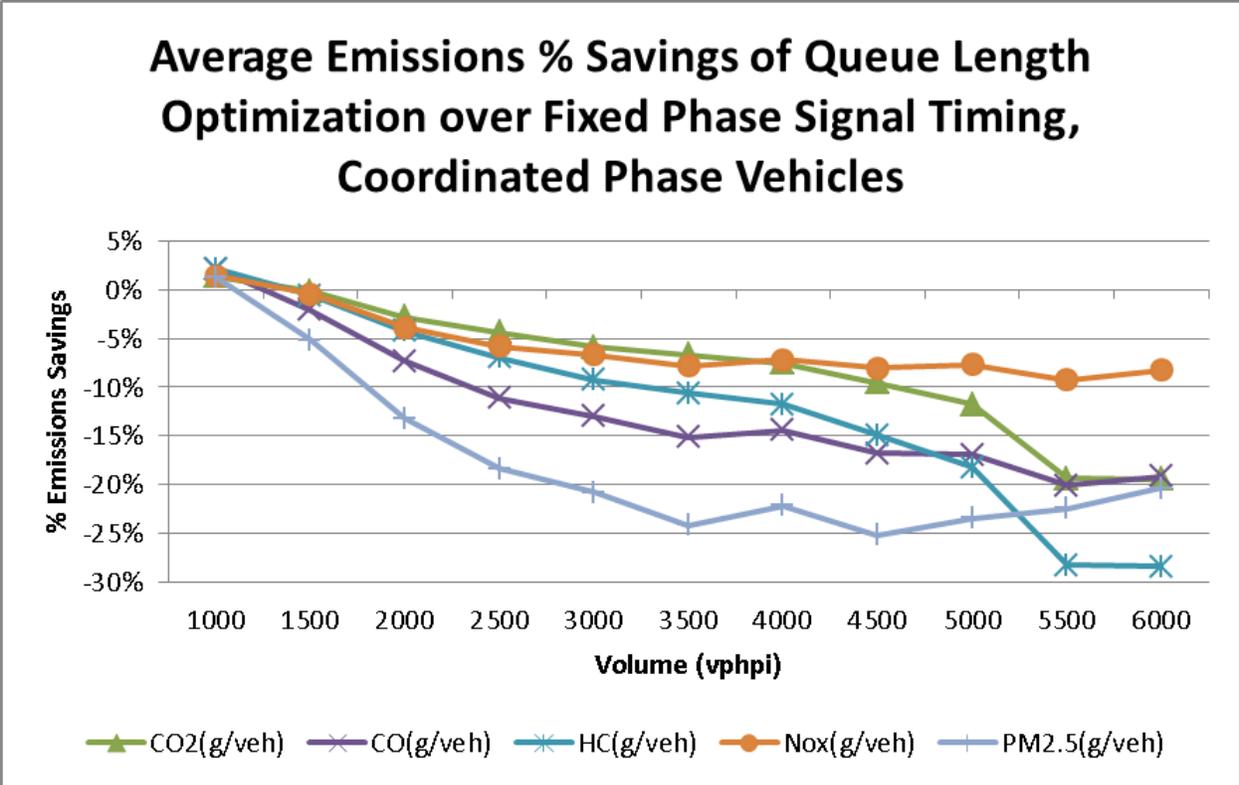
Fig. 38: Coordinated Phase Vehicle Emissions Percent Savings of Decentralized CV Queue Length Signal Optimization over Coordinated Fixed Phase Signal Timing on a 3-intersection Corridor

Table XIII: Coordinated Fixed Phase Signal Timing, Traffic Volume Sensitivity Analysis Results for Coordinated Phase Vehicles

Volume (vphpi)	Energy (kJ/veh)	CO2 (g/veh)	CO (g/veh)	HC (g/veh)	NOx (g/veh)	PM2.5 (g/veh)	VHT (s/veh)
1000	7472.2127	537.0262	10.1911	0.3290	1.2683	0.0685	130.3333
1500	7519.0645	540.3933	10.1956	0.3317	1.2741	0.0676	132.6929
2000	7486.7661	538.0720	9.9620	0.3287	1.2613	0.0650	134.3591
2500	7501.3055	539.1170	9.9366	0.3299	1.2612	0.0642	136.0377
3000	7614.5635	547.2568	10.0691	0.3351	1.2817	0.0649	138.3284
3500	7602.9540	546.4224	9.9911	0.3345	1.2758	0.0638	139.1749
4000	7695.3604	553.0636	10.1833	0.3403	1.2925	0.0654	141.6583
4500	7797.6319	560.4138	10.2841	0.3458	1.3048	0.0657	145.6000
5000	8183.8250	588.1692	10.7525	0.3683	1.3498	0.0684	162.8396
5500	8421.4687	605.2486	11.0373	0.3822	1.3790	0.0698	173.7539
6000	8739.0077	628.0699	11.3384	0.3985	1.4149	0.0715	187.3667

Table XIV: Decentralized CV Queue Length Signal Optimization, Traffic Volume Sensitivity Analysis Results for Coordinated Phase Vehicles

Volume (vphpi)	Energy (kJ/veh)	CO2 (g/veh)	CO (g/veh)	HC (g/veh)	NOx (g/veh)	PM2.5 (g/veh)	VHT (s/veh)
1000	7368.2306	529.5532	9.9716	0.3219	1.2498	0.0676	127.4682
1500	7526.7237	540.9440	10.4084	0.3336	1.2796	0.0711	131.2429
2000	7696.1421	553.1200	10.6914	0.3426	1.3102	0.0736	134.9195
2500	7830.5991	562.7833	11.0419	0.3528	1.3343	0.0760	138.4751
3000	8063.1875	579.4993	11.3743	0.3660	1.3672	0.0784	146.7799
3500	8109.6911	582.8415	11.5036	0.3699	1.3758	0.0792	147.4656
4000	8275.0532	594.7260	11.6509	0.3803	1.3849	0.0799	158.2913
4500	8540.1892	613.7811	12.0111	0.3973	1.4095	0.0822	171.9603
5000	9147.3751	657.4192	12.5736	0.4353	1.4530	0.0844	210.3675
5500	10052.5094	722.4705	13.2548	0.4904	1.5061	0.0855	272.3665
6000	10437.3531	750.1290	13.5144	0.5118	1.5318	0.0861	298.2313

Table XV: % Improvement of Decentralized CV Queue Length Optimization over Coordinated Fixed Phase Signal Timing, Traffic Volume Sensitivity Analysis Results, for Coordinated Phase Vehicles

| Volume (vphpi)	Energy (kJ/veh)	CO2 (g/veh)	CO (g/veh)	HC (g/veh)	NOx (g/veh)	PM2.5 (g/veh)	VHT (s/veh)
1000	1.39%	1.39%	2.15%	2.18%	1.46%	1.30%	2.20%
1500	-0.10%	-0.10%	-2.09%	-0.55%	-0.43%	-5.12%	1.09%
2000	-2.80%	-2.80%	-7.32%	-4.21%	-3.88%	-13.20%	-0.42%
2500	-4.39%	-4.39%	-11.12%	-6.97%	-5.79%	-18.34%	-1.79%
3000	-5.89%	-5.89%	-12.96%	-9.23%	-6.67%	-20.80%	-6.11%
3500	-6.67%	-6.67%	-15.14%	-10.59%	-7.84%	-24.18%	-5.96%
4000	-7.53%	-7.53%	-14.41%	-11.75%	-7.15%	-22.17%	-11.74%
4500	-9.52%	-9.52%	-16.79%	-14.91%	-8.02%	-25.16%	-18.10%
5000	-11.77%	-11.77%	-16.94%	-18.20%	-7.64%	-23.45%	-29.19%
5500	-19.37%	-19.37%	-20.09%	-28.29%	-9.21%	-22.50%	-56.75%
6000	-19.43%	-19.43%	-19.19%	-28.43%	-8.26%	-20.36%	-59.17%
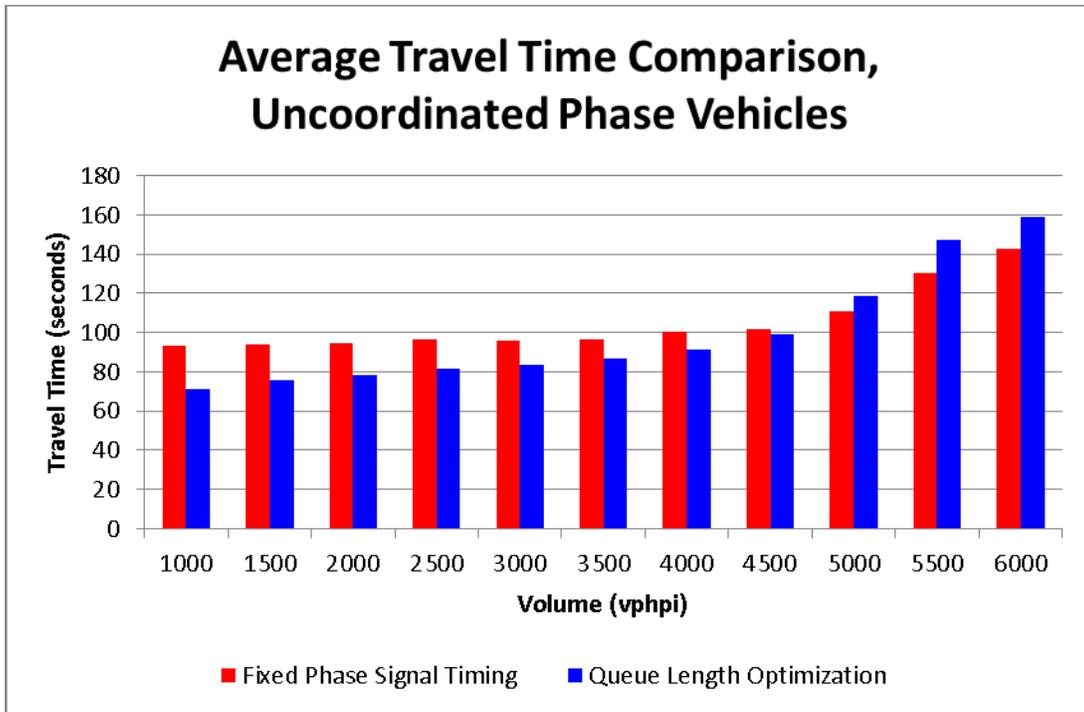
Fig. 39: Uncoordinated Phase Vehicle Travel Time Comparison of Decentralized CV Queue Length Signal Optimization and Coordinated Fixed Phase Signal Timing for a 3-intersection Corridor
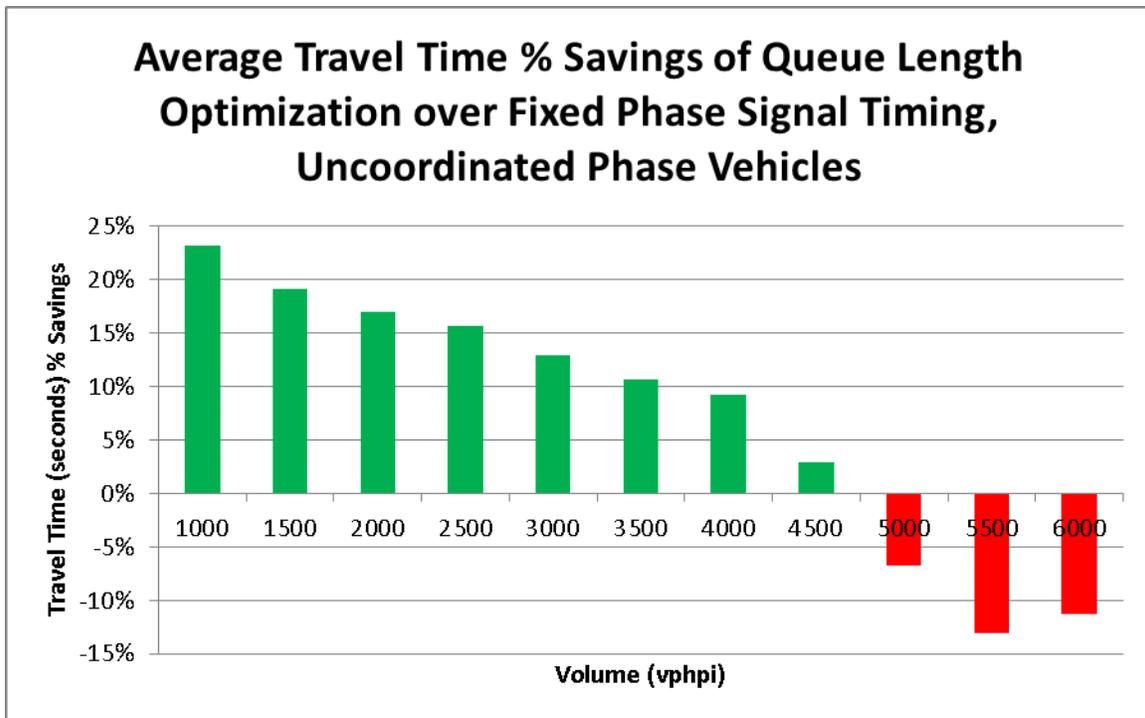

Fig. 40: Uncoordinated Phase Vehicle Travel Time Percent Savings of Decentralized CV Queue Length Signal Optimization over Coordinated Fixed Phase Signal Timing on a 3-intersection Corridor
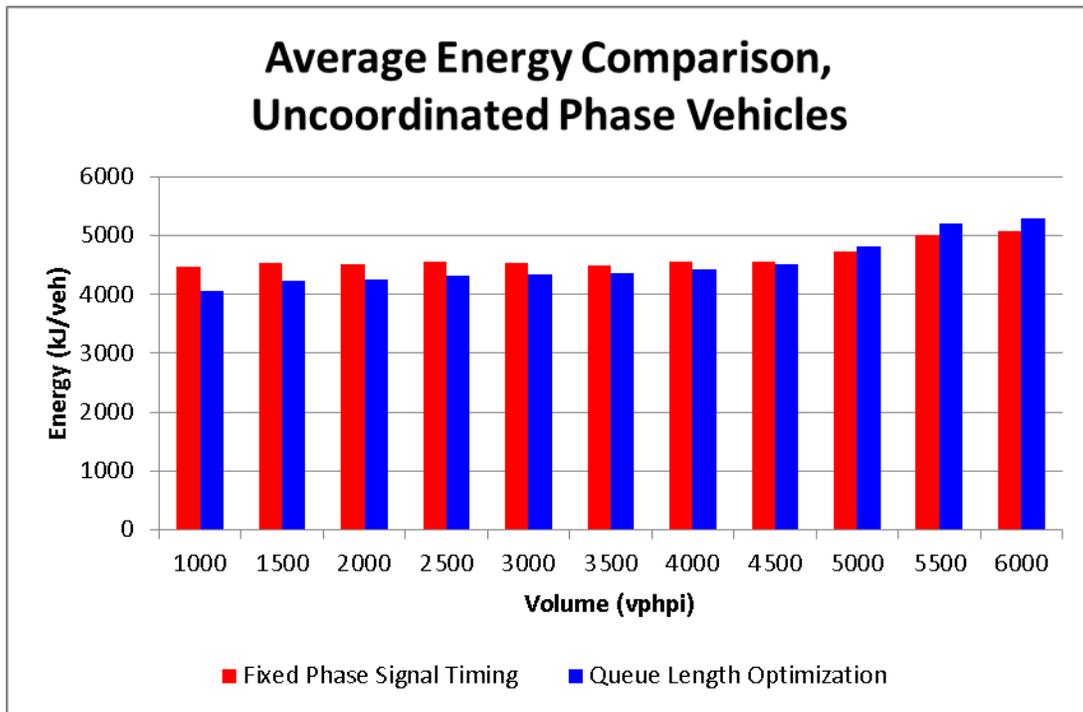
45

Fig. 41: Uncoordinated Phase Vehicle Energy Comparison of Decentralized CV Queue Length Signal Optimization and Coordinated Fixed Phase Signal Timing for a 3-intersection Corridor
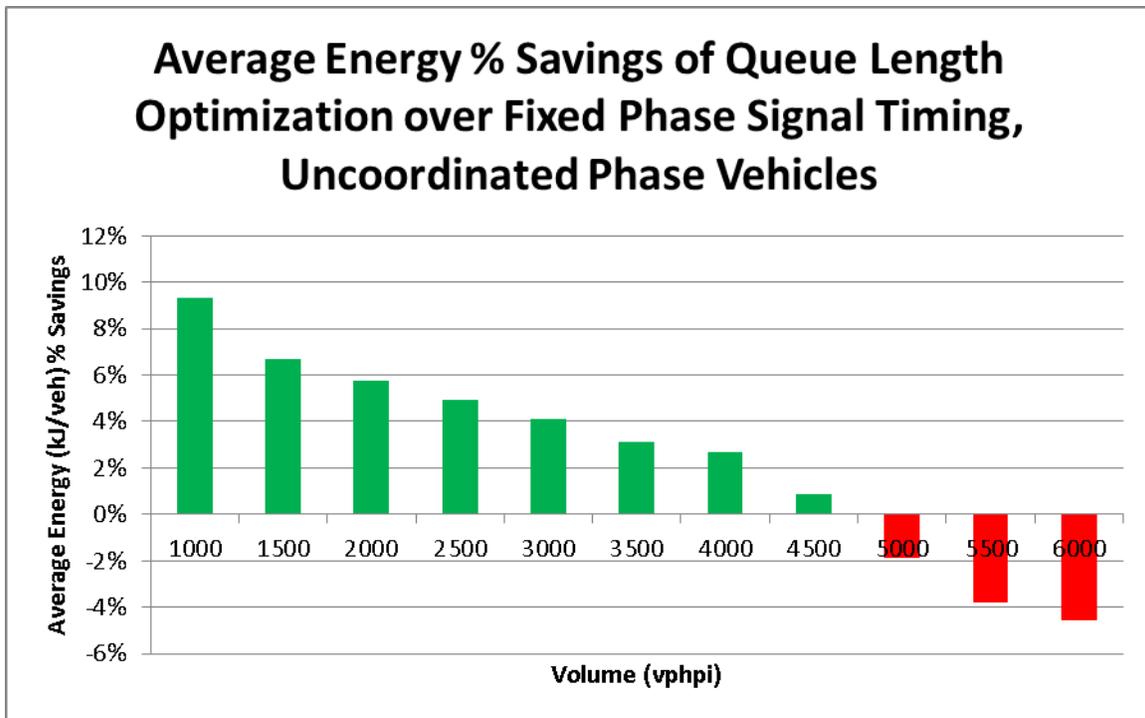

Fig. 42: Uncoordinated Phase Vehicle Energy Percent Savings of Decentralized CV Queue Length Signal Optimization over Coordinated Fixed Phase Signal Timing on a 3-intersection Corridor
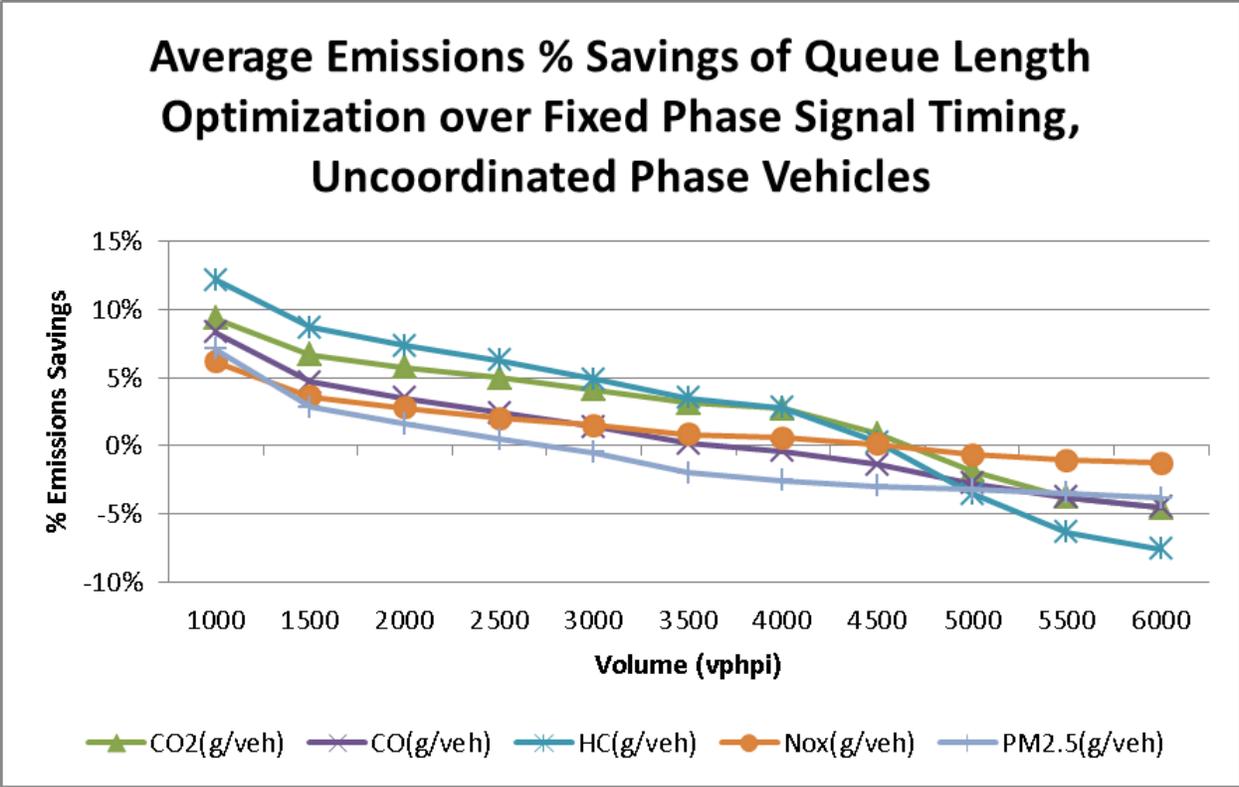
Fig. 43: Uncoordinated Phase Vehicle Emissions Percent Savings of Decentralized CV Queue Length Signal Optimization over Coordinated Fixed Phase Signal Timing on a 3-intersection Corridor

Table XVI: Coordinated Fixed Phase Signal Timing, Traffic Volume Sensitivity Analysis Results for Uncoordinated Phase Vehicles

Volume (vphpi)	Energy (kJ/veh)	CO2 (g/veh)	CO (g/veh)	HC (g/veh)	NOx (g/veh)	PM2.5 (g/veh)	VHT (s/veh)
1000	4472.8779	321.4644	6.8418	0.2152	0.7569	0.0496	93.0060
1500	4531.3534	325.6670	6.8907	0.2174	0.7664	0.0499	93.9077
2000	4517.9316	324.7024	6.8398	0.2168	0.7616	0.0494	94.4773
2500	4550.4730	327.0411	6.8464	0.2186	0.7630	0.0492	96.4714
3000	4527.7563	325.4085	6.7689	0.2169	0.7579	0.0484	96.0204
3500	4498.8905	323.3339	6.6737	0.2156	0.7493	0.0474	96.7397
4000	4550.4866	327.0421	6.6908	0.2185	0.7514	0.0472	100.3771
4500	4561.4876	327.8327	6.6579	0.2190	0.7494	0.0467	101.8819
5000	4734.1720	340.2435	6.7859	0.2284	0.7636	0.0469	111.0577
5500	5010.0231	360.0687	6.9320	0.2442	0.7775	0.0466	130.2493
6000	5071.7721	364.5065	6.8917	0.2480	0.7731	0.0456	142.4203

Table XVII: Decentralized CV Queue Length Signal Optimization, Traffic Volume Sensitivity Analysis Results for Uncoordinated Phase Vehicles

Volume (vphpi)	Energy (kJ/veh)	CO2 (g/veh)	CO (g/veh)	HC (g/veh)	NOx (g/veh)	PM2.5 (g/veh)	VHT (s/veh)
1000	4055.9481	291.5000	6.2741	0.1890	0.7102	0.0461	71.4441
1500	4228.4368	303.8967	6.5696	0.1985	0.7390	0.0485	75.9339
2000	4258.1839	306.0345	6.6025	0.2010	0.7405	0.0486	78.4212
2500	4324.9670	310.8342	6.6809	0.2049	0.7479	0.0489	81.3768
3000	4342.4276	312.0891	6.6755	0.2064	0.7466	0.0486	83.6141
3500	4357.6199	313.1809	6.6621	0.2080	0.7432	0.0483	86.4747
4000	4427.7913	318.2241	6.7171	0.2124	0.7472	0.0484	91.1646
4500	4520.8661	324.9133	6.7512	0.2184	0.7487	0.0481	98.9553
5000	4822.6587	346.6029	6.9737	0.2365	0.7687	0.0484	118.5128
5500	5200.0351	373.7247	7.1967	0.2597	0.7858	0.0482	147.2131
6000	5302.3626	381.0788	7.2019	0.2669	0.7829	0.0474	158.5766

Table XVIII: % Improvement of Decentralized CV Queue Length Optimization over Coordinated Fixed Phase Signal Timing, Traffic Volume Sensitivity Analysis Results, for Uncoordinated Phase Vehicles

| Volume (vphpi)	Energy (kJ/veh)	CO2 (g/veh)	CO (g/veh)	HC (g/veh)	NOx (g/veh)	PM2.5 (g/veh)	VHT (s/veh)
1000	9.32%	9.32%	8.30%	12.17%	6.17%	7.09%	23.18%
1500	6.68%	6.68%	4.66%	8.66%	3.57%	2.81%	19.14%
2000	5.75%	5.75%	3.47%	7.31%	2.77%	1.61%	16.99%
2500	4.96%	4.96%	2.42%	6.27%	1.97%	0.46%	15.65%
3000	4.09%	4.09%	1.38%	4.87%	1.50%	-0.51%	12.92%
3500	3.14%	3.14%	0.17%	3.51%	0.82%	-1.98%	10.61%
4000	2.70%	2.70%	-0.39%	2.76%	0.56%	-2.58%	9.18%
4500	0.89%	0.89%	-1.40%	0.25%	0.08%	-2.96%	2.87%
5000	-1.87%	-1.87%	-2.77%	-3.54%	-0.66%	-3.23%	-6.71%
5500	-3.79%	-3.79%	-3.82%	-6.35%	-1.07%	-3.48%	-13.02%
6000	-4.55%	-4.55%	-4.50%	-7.59%	-1.26%	-3.86%	-11.34%

NCST
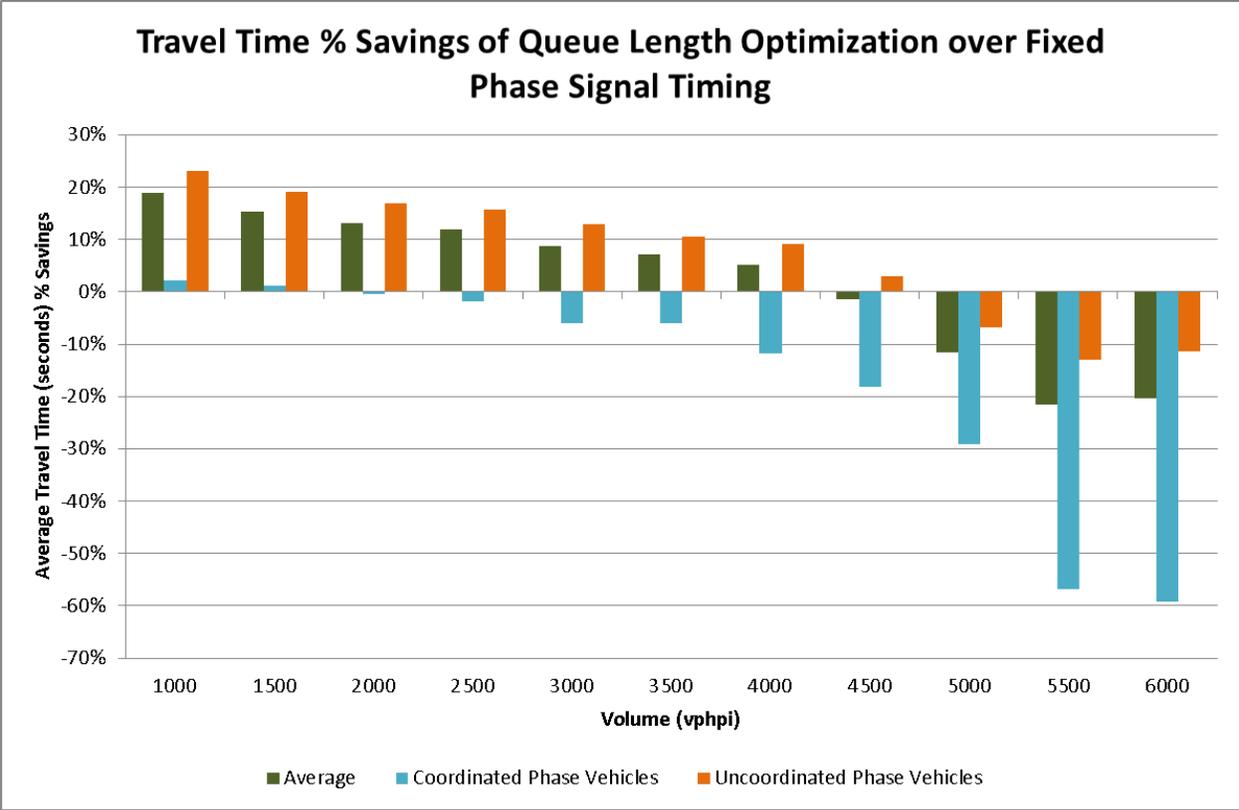
Fig. 44: Comparison of Average Travel Time Percent Savings by Category for Decentralized CV Queue Length Signal Optimization over Coordinated Fixed Phase Signal Timing on a 3-intersection Corridor
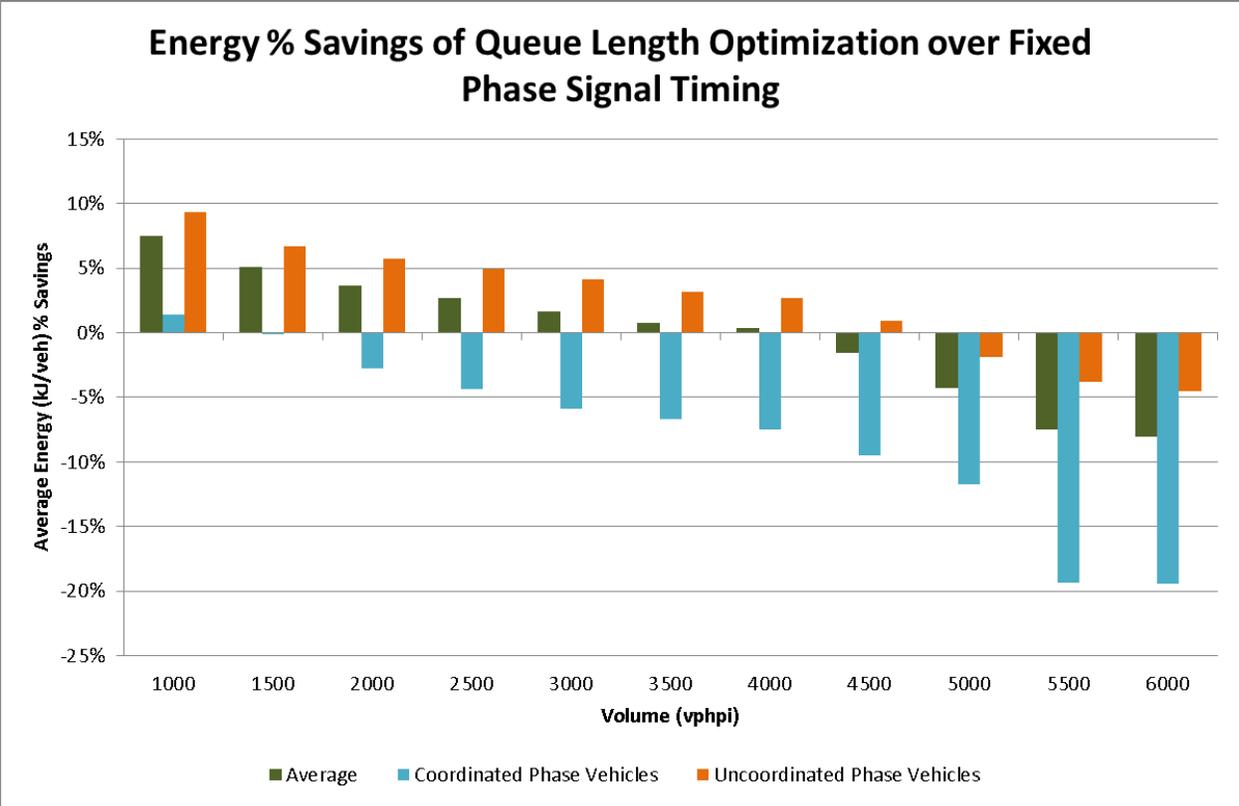
Fig. 45: Comparison of Average Energy Percent Savings by Category for Decentralized CV Queue Length Signal Optimization over Coordinated Fixed Phase Signal Timing on a 3-intersection Corridor

5. Conclusions & Future Work

In chapters 3 and 4, a CV adaptive signal control optimizer with an MOE of queue length was evaluated in the context of an isolated intersection and for a corridor of three intersections with each intersection using the same adaptive controller in a decentralized manner. For both the isolated intersection and the signalized corridor, a volume sensitivity analysis and a demand profile sensitivity analysis were conducted. In the case of the isolated intersection, the CV queue length adaptive signal control optimizer provided benefits of -1% to 33%, and 0% to 15% for average travel time and average energy, respectively, relative to a fixed phase baseline intersection. The range of benefits relative to an intersection using Webster signal timing were 0 to 13%, and 0% to 10% for average travel time and average energy, respectively. The maximum benefits provided by using the CV queue length adaptive signal control optimizer are lower relative to the Webster signal timing because the Webster signal timing baseline is given precise knowledge concerning the total incoming volume of hourly traffic, as well as from which direction each vehicle will approach the intersection. The fixed phase signal timing assumes that the ratios of vehicles using each traffic movement are known in advance. In spite of both of the baseline signal control strategies being given a priori information, the adaptive signal control strategy still provided small to moderate benefits. In addition, when compared to fixed phase signal timing, HCM signal timing, and Webster signal timing, the CV queue length adaptive signal control optimizer was the least sensitive in terms of absolute travel time.

For the case of the three-intersection corridor, the decentralized CV queue length adaptive signal control optimization strategy provided maximum benefits of 19% and 8% in terms of average travel time and average energy, respectively, relative to coordinated fixed phase signal timing. However, the positive benefits only occurred for traffic volumes less than or equal to 4000 vph. At moderate to high traffic volumes, the performance of the CV adaptive signal control strategy was counter-productive, leading to maximum penalties of up to -22% and -8% for average travel time and average energy, respectively. A further analysis of coordinated phase vehicles progressing through the length of the corridor in both the coordinated phase signal timing baseline corridor and the CV adaptive signal control corridor revealed that the coordinated phase vehicles present in the baseline network did not benefit under decentralized adaptive signal control. In contrast, vehicles not progressing through the entire length of the corridor, (uncoordinated phase vehicles), did benefit by using decentralized CV adaptive signal control for traffic volumes up to 4500 vph.

The CV adaptive signal control strategies presented in the report provides a framework for not only optimizing signal timing, but also improving environmental parameters either directly or indirectly. The environmental performance of an arterial intersection may indirectly be improved via the use of MOEs such as queue length or delay time. In addition, the environmental performance of an arterial intersection may be directly improved by permitting vehicles to communicate real-time emissions information. Furthermore, a weighted MOE may be selected in order to achieve multiple objectives (i.e. reducing travel time and reducing emissions). Individual localities can select an appropriate MOE based on their specific goals and their existing traffic patterns. For example, traffic signals along corridors which are heavily used by freight

vehicles can be optimized to provide priority for the freight vehicles. In the case of the queue length MOE, freight vehicles are effectively treated as multiple passenger vehicles by using a weighting factor (>1). The weighting factor may be increased to provide faster priority to freight vehicles. However, providing priority to freight vehicles may come at the expense of passenger vehicles. As a result, the goal of the weighting factor selection should be to improve the overall environmental performance of all vehicles entering a given intersection or corridor.

In terms of future work, one of the key areas for future exploration is addressing the question of which MOE or MOEs are the most practical and effective for deploying CV adaptive signal control optimizers in the field. The use of CV technology and the ability to transmit custom parameters from vehicles to intersections opens up a whole range of MOEs that were not possible under the traditional non-communicated paradigm. Although queue length was selected as the MOE of choice in this dissertation, it may be possible that a different MOE may provide even more substantial benefits. Other MOEs which may be explored include travel time, delay time, idling time, energy consumption, emissions, or even a weighted combination of multiple objectives. The advantage of using a weighted MOE, is that the behavior of a specific intersection can be customized based on the localities needs. Furthermore, the weights themselves can be dynamically adjusted based on real-time wind direction and air quality.

Another consideration reserved for future study is the effect of the size of the communication radius of vehicles approaching an intersection. Recall that the signal timing of the intersection is changed based on V2I information. If the radius is sufficiently large, then vehicles desiring to turn left may not yet have reached the left-turn bay. Consequently, the intersection would be unable to discern whether incoming vehicles were turning left, or continuing straight, until they reach the left-turn bay. One potential solution to the challenge is to have vehicles communicate their turning intentions via wireless messages sent to the intersection. Beyond the physical technical aspects of different communication radii, there are also application features that are affected by different communication radii. One of the open areas for research is whether a CV intersection is fully able to utilize information across a large space horizon (a large communication radius). Even if a vehicle can communicate with a given intersection at a distance of 1000 meters, the intersection may not be able to make practical use of that information due to the large distance, and thus long time duration before the vehicle arrives at the intersection. As a result, the intersection may employ its own effective "receiving" radius, where it only considers vehicles that are within a certain range of the intersection.

For the signalized corridor, although the decentralized CV adaptive signal strategy did show moderate benefits, it is likely that the approach must be modified before deployment due to the current poor performance at traffic volumes greater than 4000 vph. A logical next step would be to test a centralized CV adaptive signal control strategy in which adjacent intersection communicate information which helps to optimize a stated network objective such as average network travel time. Furthermore, the strategy can be scaled to be applied to a grid network of intersections. In the case of applying a centralized CV adaptive signal control strategy to a grid network, a given intersection would communicate with up to 4 adjacent intersections.

Furthermore, for the health and safety of pedestrians and residents, freight vehicles could be routed around the periphery of a grid network of intersections.

References

[1] D. Schrank, B. Eisele and T. Lomax. "TTI's 2012 Urban Mobility Report". Dec. 2012.

[2] "Inventory of U.S. Greenhouse Gas Emissions and Sinks: 1990-2012". U.S. Environmental Protection Agency. April 2014.

[3] "National Transportation Statistics". U.S. Department of Transportation (USDOT). 2014.

[4] Highway Capacity Manual 2010 (HCM 2010). Transportation Research Board, 2011.

[5] Traffic Detector Handbook: Third Edition. Federal Highway Administration (FHWA), FHWA-HRT-06-108, Oct. 2006.

[6] "Report and Order FCC-03-324," Federal Communications Committee. Feb. 2004.

[7] J. Guo and N. Balon. "Vehicular Ad Hoc Networks and Dedicated Short Range Communication," University of Michigan, Dearborn. June 2006.

[8] N. Goodall. "Traffic Signal Control with Connected Vehicles". Ph. D. Thesis, University of Virginia, May 2013.

[9] H. Rakha, et al.. "Traffic Signal Control Enhancements under Vehicle Infrastructure Integration Systems". Final report, MAUTC-2008-02, Dec. 2011.

[10] Q. He, L. Head and J. Ding. "PAMSCOD: Platoon-based Arterial Multi-modal Signal Control with Online Data". Procedia Social and Behavioral Sciences, 17, 2011, pp. 462 – 489.

[11] L-W Chen, P. Sharma and Y-C Tseng. "Dynamic Traffic Control with Fairness and Throughput Optimization using Vehicular Communications". IEEE Journal on Selected Areas in Communications/Supplement, Vol. 31, No. 9, 2012, pp. 504 – 512.

[12] D. Kari, G. Wu and M. Barth. "Eco-Friendly Freight Signal Priority Using Connected Vehicle Technology: A Multi-Agent Systems Approach". IEEE on Intelligent Vehicle Symposium, June 2014.

[13] NEMA: National Electrical Manufacturers Association, The Association of Electrical Equipment and Medical Imaging Manufacturers. [Online]. Available: http://www.nema.org/pages/default.aspx

[14] "Signal Timing on a Shoestring," U.S. Department of Transportation Federal Highway Administration. Washington, DC: 2005.

[15] A. Stevanovic. "Adaptive Traffic Control Systems: Domestic and Foreign State of Practice – A Synthesis of Highway Practice". NCHRP Synthesis 403, 2010.

[16] D. I. Robertson. "TRANSYT Method for Area Traffic Control". Traffic Engineering and Control, Vol. 11, No. 6, 1969, pp. 276 – 281.

[17] N. H. Gartner, and R. M. Deshpande. "A Dynamic Programming Approach for Arterial Signal Optimization". Presented at the 92nd TRB Annual Meeting, Jan. 2013.

[18] Signal Timing Manual, U.S. Department of Transportation Federal Highway Administration, Washington, DC, 2008, pp. 63-71.

[19] Quadstone, Paramics, 2016. http://www.paramics-online.com/.

[20] "MOtor Vehicle Emission Simulator (MOVES) Version 2010b," USEPA, 2011.